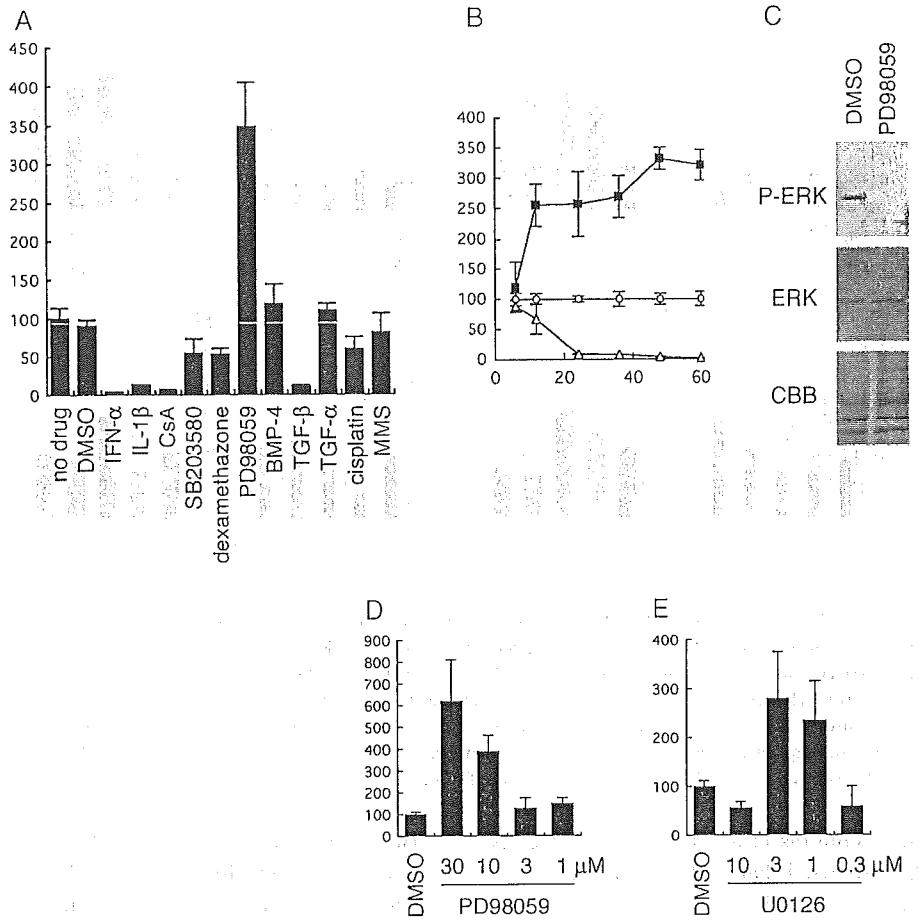

Fig. 2. Increased luciferase-replicon by PD98059 or U0126. (A) curedMH14 cells transfected with the luciferase-replicon RNA construct (LMH14) were treated with DMSO (0.1%), IFN-α (100 IU/ml), IL-1β (10 ng/ml), cyclosporin A (CsA, 1 μg/ml), SB203580 (10 μM), dexamethazone (1 μM), PD98059 (10 μM), BMP-4 (10 ng/ml), TGF-β (2 ng/ml), TGF-α (1 ng/ml), cisplatin (1 μg/ml) or MMS (methyl methanesulfonate; 0.1 mM). Three days later, cellular luciferase activity was measured. (B) curedMH14 cells transfected with the luciferase-replicon RNA construct were treated with DMSO (white circle), PD98059 (10 μM, black box) or IFN-α (100 IU/ml). At the indicated times, cells were harvested for determination of luciferase activity. The activity of DMSO-treated cells was set to 100%. (C) Western blotting analysis of phospho-ERK (upper panel) and total ERK (middle panel) in cells treated with or without PD98059 (10 μM) for 10 h. CBB staining pattern of the same blot is used as a loading control (lower panel). (D,E) Dose-dependence of MEK–ERK inhibitors on the activity of the luciferase-replicon. Cells transfected with the luciferase-replicon RNA construct were treated with varying concentrations of PD98059 (D) or U0126 (E), and luciferase activity was subsequently determined. The luciferase activity was shown with the SD value of three independent experiments.

response to growth or stress signals, respectively, and MNK phosphorylates eIF4E (Raught and Gingras, 1999).

Cell treatment with 20 μM CGP57380 decreased the luciferase-replicon to 34% (Fig. 4A) and the ratio of IRES-dependent over cap-dependent value to 64% when di-cistronic vector (Fig. 4B) was used. There was little to no effect of lower inhibitor concentrations on translation (Figs. 4A,B,C). In order to verify the effectiveness of CGP57380, we examined the activation of eIF4E by blotting with an anti-phospho-eIF4E antibody. Treatment with CGP57380 clearly eliminated eIF4E phosphorylation, and a partial reduction in eIF4E phosphorylation was seen following treatment with PD98059, even though total eIF4E levels were unchanged (Fig. 4D).

These data, combined with accumulating evidence (Scheper and Proud, 2002), suggest that eIF4E phosphorylation does not play a positive role in cap-dependent translation, and, moreover, it may limit cap-dependent translation in cultured cells, although the physiological significance of eIF4E phosphorylation remains controversial. Nevertheless, drug-induced reduction in eIF4E phosphorylation did not enhance IRES-dependent translation compared to cap-dependent translation.

Effect of 4EBP on HCV IRES

An additional key translation regulator downstream of the MEK–ERK pathway is the eIF4E-binding protein 4EBP. When eIF4E is bound by 4EBP, ribosomes are not recruited to the cap structure and translation is blocked. Among the three isoforms, 4EBP1 is the best characterized. The binding of 4EBP1 with eIF4E is controlled by the phosphorylation state of 4EBP1, where the hypo/basal-phosphorylated form of 4EBP1 interacts tightly with eIF4E, but upon hyper-phosphorylation, 4EBP1 binding to eIF4E is inhibited (Gingras et al., 2001). mTOR has been reported to

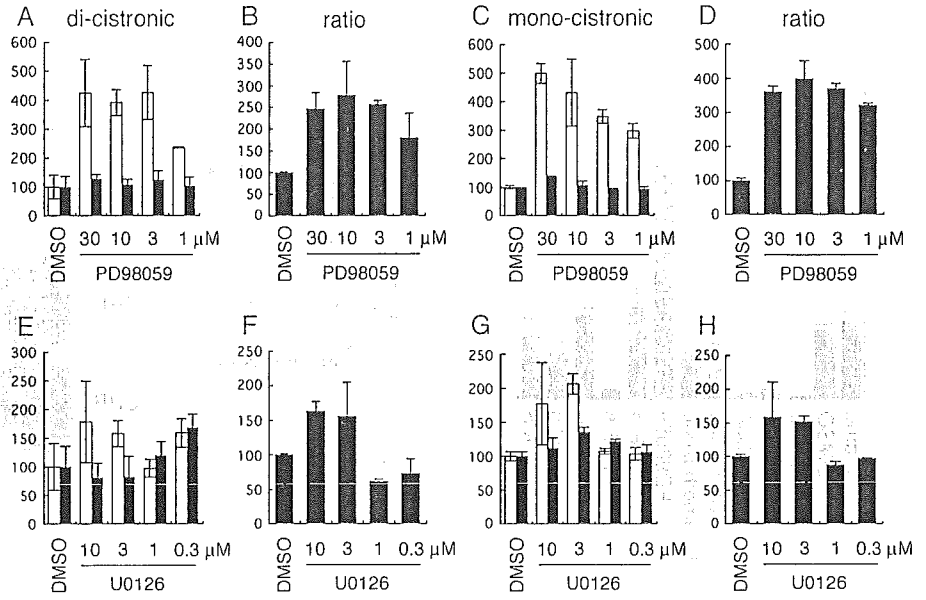

Fig. 3. Increased HCV IRES by PD98059 or U0126. Dose-dependence of MEK–ERK inhibitors on the activity of the di-cistronic pRLIL-2 vector (A,B,E,F) and mono-cistronic expression vectors (C,D,G,H). (A,E) Cells transfected with di-cistronic pRLIL-2 were incubated with varying concentrations of PD98059 (A) or U0126 (E), and luciferase activity was subsequently determined. IRES-dependent firefly luciferase activity is shown in white, and cap-dependent renilla luciferase activity is in black. (B,F) The results in panels (A) and (E) are shown as the ratio of IRES-dependent over cap-dependent value, respectively. (C,G) Cells transfected with mono-cistronic IRES-luc (white bar) and cap-rluc-pA (black bar) were incubated with varying concentrations of PD98059 (C) or U0126 (G), and luciferase activity was subsequently determined. (D,H) The results in panels (C) and (G) are shown as the ratio of IRES-dependent over cap-dependent value, respectively. The luciferase activity was shown with the SD value of three independent experiments.

phosphorylate 4EBP1 (Gingras et al., 1999), and, recently, Herbert et al. (2002) proposed that ERK is involved in the hyper-phosphorylation of 4EBP1.

We investigated a possible role for 4EBP1 in the observed IRES activation by PD98059. Exogenous expression of wild type or dominant active form of 4EBP1 (T46A, Mothe-Satney et al., 2000) elevated the luciferase-replicon to 420 and 325% of control levels, respectively, and PD98059 treatment enhanced these effects (Fig. 5A). A mutant form of 4EBP1 unable to interact with eIF4E (mBD, Mader et al., 1995), however, did not affect the luciferase-replicon activity (Fig. 4A). Luciferase expression driven by a di-cistronic vector resulted in a similar trend (Fig. 5C). Both the wild type and mBD forms of 4EBP1 were hyper-phosphorylated (Fig. 5D). In the cell line used, Huh-7, endogenous 4EBP1 was not detected (Fig. 5D, vec). The expression levels of wild-type and T46A were reduced compared to mBD, likely as a result of the auto-suppression of cap-dependent translation by the wild type or T46A 4EBP1.

We next tried to eliminate endogenous 4EBP. Knock-down of 4EBP was confirmed following individual siRNA (Fig. 6A) or all siRNAs treatment (Fig. 6B). Among the different 4EBP isoforms, knock-down of 4EBP2 led to the strongest reduction in the luciferase-replicon (Figs. 6C,D) and the IRES/cap-translation in the di-cistronic vector (Figs.

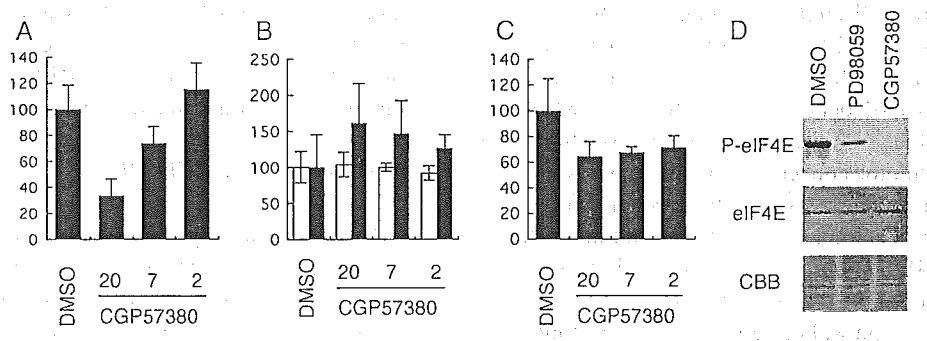

Fig. 4. Effect of CGP57380 on luciferase-replicon or HCV IRES. (A) Cells transfected with the luciferase-replicon RNA construct were treated with CGP57380 (μM). Three days after transfection, cells were harvested for determination of luciferase activity. The activity of DMSO-treated cells was set to 100%. (B) Cells transfected with di-cistronic pRLIL-2 were incubated with CGP57380, and luciferase activity was subsequently determined. IRES-dependent firefly luciferase activity is shown in white, and cap-dependent renilla luciferase activity is in black. (C) The results in panel (B) are shown as the ratio of IRES-dependent over cap-dependent value. The luciferase activity was shown with the SD value of three independent experiments. (D) Western blotting was performed to examine the phosphorylation of eIF4E (upper panel) and total eIF4E (middle panel) in cells treated with or without CGP57380 (20 μM). CBB staining pattern of the same blot is used as a loading control.

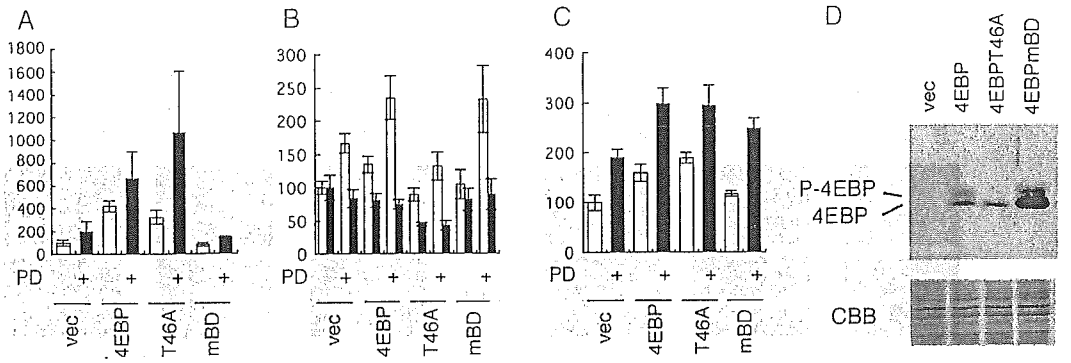

Fig. 5. Effect of exogenous expression of 4EBP on luciferase-replicon or HCV IRES. (A) Cells were transfected with the luciferase-replicon RNA construct together with empty vector (vec), vector for 4EBP1, 4EBP1T46A or 4EBP1mBD. 4EBP1T46A is a dominant-active form of 4EBP1, and 4EBP1mBD lacks the ability to bind with eIF4E. Cells were harvested for determination of luciferase activity after 3 days incubation with PD98059 (10 μM). White and black bars indicate absence and presence of PD98059, respectively. The data are normalized by cotransfection with the pRL-TK. (B) Cells were cotransfected with dicistronic pRLIL-2 together with empty vector (vec), vector for 4EBP1, 4EBP1T46A or 4EBP1mBD. Luciferase activity was subsequently determined. IRES-dependent firefly luciferase activity is shown in white, and cap-dependent renilla luciferase activity is in black. (C) The results in panel (B) are shown as the ratio of IRES-dependent over cap-dependent value. White and black bars indicate absence and presence of PD98059, respectively. The luciferase activity was shown with the SD value of three independent experiments. (D) Western blotting was performed to examine the expression and phosphorylation state of 4EBP in cells using anti-4EBP antibody. CBB staining pattern of the same blot is used as a loading control.

6G,H). Huh-7 cells express higher levels of 4EBP2 compared to the other isoforms, and we hypothesize that this may account for the observed effect.

The above results suggest that 4EBP proteins, particularly 4EBP2 in this cell line, play an important role in HCV IRES-mediated translation. However, no evidence implicated 4EBP in the ERK-mediated modification of IRES activity because, even in the presence of the mBD mutant or the elimination of 4EBP isoforms, PD98059-mediated activation of IRES-dependent translation still occurred.

Effect of PD98059 on G418-resistant subgenomic replicon

Since IRES-mediated translation can regulate RNA replication in cultured HCV replicon cells (He et al., 2003), we tested the effect of PD98059 on G418-resistant replicon RNA replication. When monitored by either real-time RT-PCR (Fig. 7A) or Northern blotting (Fig. 7C), replicon RNA was increased up to 210% of vehicle-treated control by the administration with 30 μM of PD98059 for 24 h. The replicon RNA levels decreased at 48 h or later probably because of the cell growth suppression (Fig. 7B). Additionally, PD98059 induced the production of viral protein NS5A (Fig. 7D). Although replicon RNA levels can fluctuate and are not the most stringent test, as Zhu and Liu (2003) also observed, the observed up-regulation of HCV replicon RNA and a viral protein at 24 h strongly suggests an effect of PD98059.

PD9805 promotes HCV multiplication in a model of HCV infection

To examine the effects of PD98059 on HCV replication, we infected curedMH14 (Fig. 8A), Huh-7 (B), OUMS-29 H-11 (C) or PH5CH8 (D) cells with HCV-positive serum for 1 day and incubated cells with either PD98059 or vehicle. curedMH14 had been prepared by curing an HCV replicon cell line of replicon RNA (Murata et al., 2005). OUMS-29/H-11 is a human hepatocyte cell line, in which SV40 large T antigen and hepatocyte nuclear factor 4 (HNF4) had been introduced by stable transfection (Inoue et al., 2001), and PH5CH8 is a human hepatocyte line that hat had been immortalized with SV40 large T antigen (Ikeda et al., 1998).

HCV replication efficiency is highly dependent on the cell culture conditions, and poor infectivity can lead to little or no replication. However, HCV infectivity was dramatically improved by the addition of 30 μM PD98059 (Fig. 8). With 30 μM PD98059, virus RNA levels on day 5 were 162, 113 and 146% of the levels of day 1, whereas they were 0, 33 and 0% in curedMH14, OUMS-29 H-11 and PH5CH8 cells treated with DMSO, respectively. Thus, HCV replication was increased by 100-fold or more in curedMH14 and PH5CH8 cells on the fifth day. Huh-7 cells were not as permissive for viral infection under these conditions.

Discussion

In this study, we found that the addition of PD98059, an inhibitor of the MEK–ERK pathway, enhanced HCV IRES-dependent translation and HCV replication in cultured cells.

Multiple cellular factors bind directly to the HCV IRES including eIF3 (Sizova et al., 1998), the 40S ribosome (Otto et al., 2002), polypyrimidine tract-binding protein (PTB, Ali and Siddiqui, 1995), La autoantigen (Ali and Siddiqui, 1997) and heterogeneous nuclear ribonucleoprotein L (hnRNP L, Hahm et al., 1998). Some of these molecules may play a role in the PD98059-mediated activation of HCV IRES-dependent translation.

Several reports have suggested that translation driven by the HCV IRES (Honda et al., 2000), as well as other IRESes (Pyronnet et al., 2000; Cornelis et al., 2000), is highest in

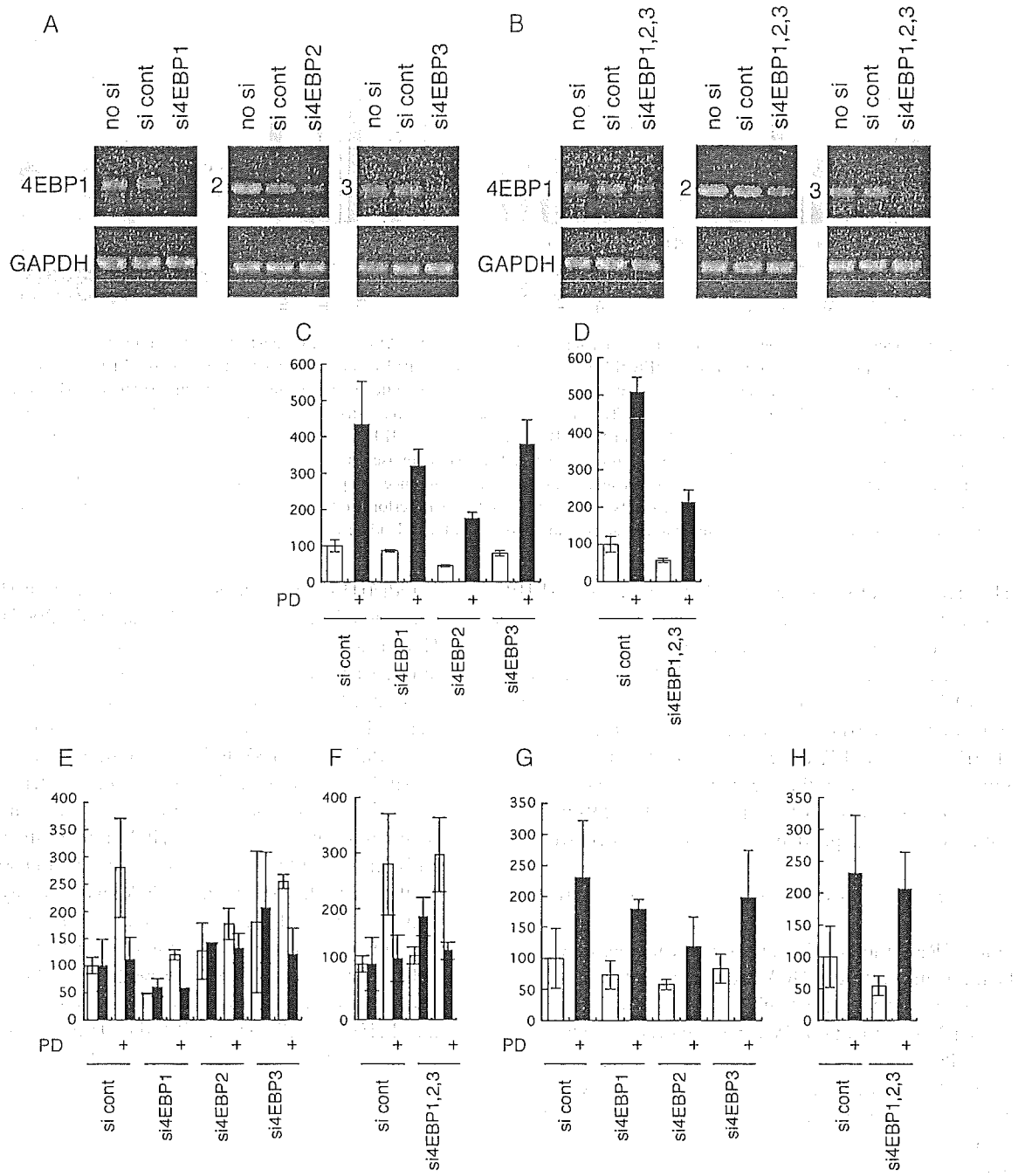

Fig. 6. Effect of RNAi knock-down of 4EBPs on luciferase-replicon or HCV IRES. (A) Cells were transfected with control siRNA (si cont) or si4EBP1, 2 or 3, independently. Total RNA was collected to examine the levels of relevant 4EBP RNA by RT-PCR. (B) Cells were transfected with control siRNA (si cont) or si4EBP1, 2 and 3, altogether. Total RNA was collected to examine the levels of every isoform of 4EBP RNA by RT-PCR. (C,D) Cells were cotransfected with LMH14 luciferase-replicon RNA construct and various siRNAs, independently (C) or together (D). Luciferase activity was determined after 3 days incubation with or without 10 μM PD98059. White and black bars indicate absence and presence of PD98059, respectively. The data are normalized by cotransfection with the pRL-TK. (E,F) Cells were cotransfected with di-cistronic pRLIL-2 together with various siRNAs, independently (E) or together (F). Luciferase activity was subsequently determined. IRES-dependent firefly luciferase activity is shown in white, and cap-dependent renilla luciferase activity is in black. (G,H) The results in panels (E) and (F) are shown as the ratio of IRES-dependent over cap-dependent value. White and black bars indicate absence and presence of PD98059, respectively. The luciferase activity was shown with the SD value of three independent experiments.

the mitotic phase (G2/M) and relatively lower in other phases of the cell cycle. Since the MEK–ERK signaling pathway is largely suppressed in the G2 phase (Tamemoto et al., 1992), MEK–ERK signaling may also be a key regulator of this phenomenon.

In addition to ERK signaling, p38 MAPK and JNK signaling pathways are also involved in translation regulation. Cellular stress negatively affects cap-dependent protein synthesis (Patel et al., 2002), while EMCV (Hirasawa et al., 2003) or c-*myc* (Subkhankulova et al., 2001) IRES-

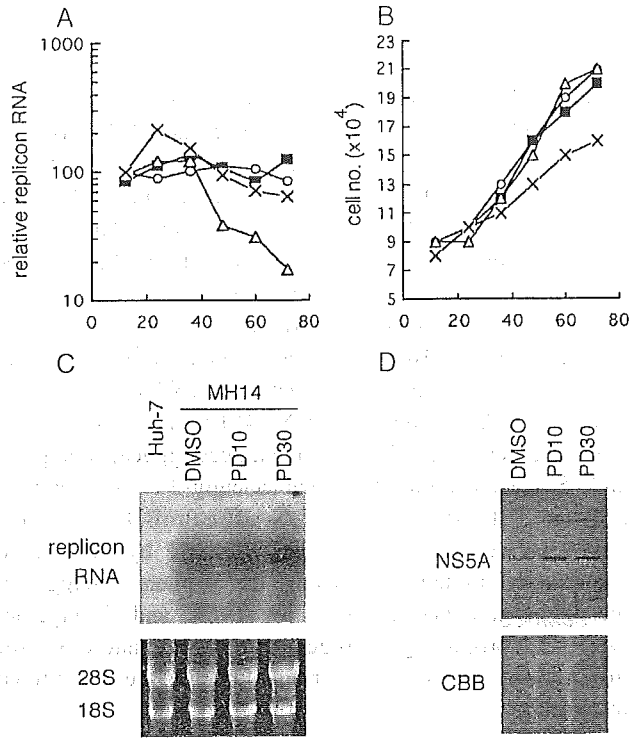

Fig. 7. Effect of PD98059 on G418-resistant subgenomic replicon. (A) MH14, a G418-resistant subgenomic replicon cell line, was treated with DMSO (white circle), 30 μM PD98059 (X), 10 μM PD98059 (black box) or 100 IU/ml IFN-α (white triangle) for 1, 3, 5 or 7 days. Following the extraction of total RNA, the quantity of HCV replicon RNA was determined by real-time RT-PCR analysis. (B) In parallel with the experiments in Fig. 5A, cells were treated with DMSO (white circle), 30 μM PD98059 (X), 10 μM PD98059 (black box) or 100 IU/ml IFN-α (white triangle). Cell numbers were counted at the indicated time points. (C) Total RNA of cells treated for 1 day was also subjected to Northern blot analysis (upper panel). The ethidium bromide staining of ribosomal RNA is shown as an internal control (lower panel). (D) Total protein of cells treated for 1 day was harvested to examine the amount of NS5A (upper panel). CBB staining pattern of the same blot is shown as a loading control (lower panel).

dependent translation is elevated by these signals. Therefore, these signaling pathways may also affect HCV IRES-dependent translation.

A cell culture system supporting HCV replication has not existed for some time. When immortalized hepatocyte cell lines are infected with HCV, viral replication efficiency is not high despite high replication rates in patients. Many researchers have attempted to solve this problem. Ikeda et al. (1998) demonstrated that incubation of cells at lower temperature helps virus replication. Aizaki et al. (2003) used a three-dimensional hepatocyte culturing system. Others varied the bovine serum levels, vitamins, lipids or amino acid composition or the pH of the culture medium. We observed that freshly thawed cells with lower viability supported replication better than rapidly growing cells. We now propose a simple infection system that supports highly efficient HCV replication in cultured cells by adding PD98059 in the medium.

Cells isolated from human liver are cultured in conditions that substantially differ from the in vivo environment and are often immortalized by oncogene expression. Consequently, many signaling pathways are likely aberrantly regulated in vitro. Among these pathways, it seems likely that ERK signaling is responsible for regulating HCV replication in cultured cells, and PD98059 may help mimic the in vivo environment and facilitate HCV replication by enhancing IRES-dependent translation.

Although treatment with PD98059 increased the replication of viral RNA in various cell lines when infected with HCV-positive serum (Fig. 8), replicon RNA levels were not increased under similar conditions (Fig. 7). The RNA copy number may explain these differences. PD98059 may not enhance the replication of replicon RNA because, in these systems, viral RNA and proteins are abundant even in the absence of the inhibitor. In cells infected with patient serum, highly efficient IRES-dependent translation may be essential for viral replication due to the low copy number of viral RNA per cell.

Mutations of serine residues within NS5A that affect the protein hyper-phosphorylation enhance replication of the virus replicon (Blight et al., 2000), and inhibitors of NS5A kinase(s) activate replication (Neddermann et al., 2004). Since the CMGC group of serine–threonine kinases has been implicated in the phosphorylation of NS5A (Reed et al., 1997), PD98059 might affect the

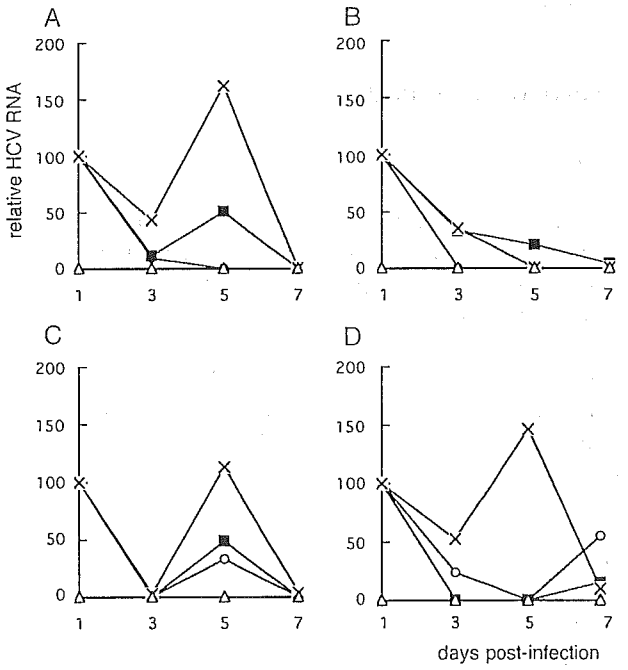

Fig. 8. Increased HCV multiplication by PD9805 in cells infected with HCV-positive serum. curedMH14 (A), Huh-7 (B), OUMS-29 H-11 (C) or PH5CH8 (D) cells were infected or mock-infected (white triangle) with HCV-positive serum for 1 day. After extensive washing with PBS, the cells were cultured with fresh medium supplemented with DMSO (white circle), 30 μM PD98059 (X), 10 μM PD98059 (black box). At the indicated times, total RNA was extracted, and the quantity of HCV RNA was determined by real-time RT-PCR analysis.

phosphorylation of the NS5A protein and thereby elevate replication. When we treated cells with PD98059, however, the levels of hyper-phosphorylated NS5A were not affected (not shown). This suggests that PD98059 activates viral replication through the enhancement of IRES-mediated translation but not through a reduction in phosphorylation state of NS5A.

Multiplication of influenza virus (Pleschka et al., 2001), borna disease virus (Planz et al., 2001), coxsackievirus (Luo et al., 2002), visna virus (Barber et al., 2002), human immunodeficiency virus (Montes et al., 2000), vaccinia virus (de Magalhaes et al., 2001), Epstein–Barr virus (Gao et al., 2001), cytomegalovirus (Rodems and Spector, 1998) and human herpesvirus-8 (Akula et al., 2004) are promoted by MEK–ERK signaling pathway activation. Activation of this pathway results in efficient cell cycle promotion, high cellular or viral gene production and increased availability of biomaterials, such as nucleotides or amino acids. Many of these viruses, therefore, likely exploit the cellular environment created through the activation of the MEK–ERK pathway. Interestingly, replication of the hepatitis B virus (HBV) is negatively regulated by the MAPK signaling pathway (Zheng et al., 2003). Because both HBV and HCV infect the same target organ, it is possible that both viruses have evolved similar means to exploit host signaling pathways. Much research is needed to identify the factors conferring organ specificity to HCV, however.

Materials and methods

Cell culture, antibodies and reagents

Huh-7 or curedMH14 cells (Murata et al., 2005) were maintained in Dulbecco's modified Eagle medium (Invitrogen, Carlsbad, CA) supplemented with 10% fetal bovine serum, 100 units/ml nonessential amino acids (Invitrogen, Carlsbad, CA) and 100 μg/ml penicillin and streptomycin sulfate (Invitrogen, Carlsbad, CA). MH14 replicon cells (Miyanari et al., 2003) were cultured in the same medium with 300 μg/ml G418 (Geneticin, Invitrogen, Carlsbad, CA). OUMS-29/H-11 cells (Inoue et al., 2001, Fukaya et al., 2001) were maintained in ASF-104 medium (Ajinomoto, Tokyo, Japan) with 100 μg/ml penicillin and streptomycin sulfate (Invitrogen, Carlsbad, CA), and PH5CH8 cells were cultured as described (Ikeda et al., 1998).

Rabbit anti-ERK, rabbit anti-phospho-ERK, rabbit anti-eIF4E and mouse anti-phospho-eIF4E antibodies were purchased from Cell Signaling Technology (Beverly, MA). Rabbit anti-4EBP antibody was from Santa Cruz Biotechnology (Santa Cruz, CA). Horseradish-peroxidase-linked goat antibodies to mouse or rabbit IgG were from Amersham Biosciences (Piscataway, NJ). PD98059 and other inhibitors were obtained commercially from Calbiochem-Novabiochem (San Diego, CA).

Plasmid construction

The pLMH14, used to synthesize the luciferase-replicon LMH14 RNA and mono-cistronic IRES-luc RNA, has been described previously (Murata et al., 2005). The di-cistronic plasmid vector, pRLIL-2, was based on the pRL-CMV Vector (Promega, Madison, WI) and contains HCV IRES sequence (complete 5′-UTR sequence and initial part of the Core gene) plus the firefly luciferase sequence obtained from pGL2 Vector (Promega, Madison, WI).

The human 4EBP1 gene was cloned by RT-PCR into the mammalian expression vector pcDNA3 (Invitrogen, Carlsbad, CA) to obtain pcDNA4EBP. Primers used to clone the gene were 5′-cggaattcgatgtccgggggcagcagctgc-3′ and 5′-ctgactcgagttaaatgtccatctcaaactgtg-3′. To generate pcDNS4EBPT46A and pcDNA4EBPmBD plasmids, mutations were inserted into pcDNA4EBP by PCR-based site-directed mutagenesis using the primers 5′-ctggtacc-tcccggggcggtgctgaagagcgtg-3′ for T46A and 5′-gaggtac-caggatcatc**tat**gaccggaaa**ttc**gcggcggagtgtcggaactc-3′ for mBD. Bold letters in the primers denote the substituted nucleotides.

RNA synthesis in vitro

In order to synthesize the LMH14 luciferase-replicon RNA or mono-cistronic IRES-luc RNA, pLMH14 was digested with *Xba*I or *Kpn*I, respectively, and subjected to in vitro transcription using a MEGAscript T7 kit (Ambion, Austin, TX) according to the manufacturer's instructions. Following DNase treatment, RNA was purified by lithium chloride precipitation. For production of mono-cistronic cap-rluc-pA RNA, the pRL-TK Vector (Promega, Madison, WI) was cut with *Xba*I and transcribed in vitro using mMESSAGE mMACHINE T7 Kit (Ambion, Austin, TX) for capping. Poly(A) Tailing Kit (Ambion, Austin, TX) was then used for polyadenylation of the RNA.

Luciferase assay

Lipofection with RNA was performed using DMRIE-C reagent (Invitrogen, Carlsbad, CA) according to the manufacturer's instructions. Plasmid DNA, including pRLIL-2, was transfected into cells using FuGENE6 reagent (Roche, Indianapolis, IN). Luciferase activity was measured using a Dual-Luciferase Reporter Assay System (Promega, Madison, WI). Assays were performed in triplicate; standard deviations are denoted by bars in the figures.

Real-time RT-PCR analysis

Total RNA was extracted from cells using Sepasol RNAI super reagent (Nacalai Tesque, Kyoto, Japan) according to the manufacturer's protocol. The 5′-UTR of HCV genomic RNA was quantified with the ABI PRISM 7700 sequence detector (Applied Biosystems, Foster City,

CA) as described (Watashi et al., 2003) using the 5′-CGGGAGAGCCATAGTGG-3′ (forward) and 5′-AGTAC-CACAAGGCCTTTCG-3′ (reverse) primers and the fluorogenic probe 5′-CTGCGGAACCGGTGAGTACAC-3′. As an internal control, ribosomal RNA was quantified using TaqMan ribosomal RNA control reagents (Applied Biosystems, Foster City, CA).

Northern and Western blot analysis

Total RNA was extracted from cells using Sepasol RNAI super reagent (Nacalai Tesque, Kyoto, Japan). Northern or Western blot analysis was performed as described previously (Kishine et al., 2002). The 1.5-kb *Eco*RI fragment of pNNRZ2 was used as the probe, which corresponds to the C-terminal half of the NS5A gene and N-terminal half of the NS5B gene.

In vitro HCV infection

The in vitro HCV infection experiment was carried out as described previously (Watashi et al., 2003). In short, cells were infected with the serum which was prepared from an HCV-positive blood donor. At 24 h post-inoculation, the cells were washed three times with PBS and maintained with fresh medium with DMSO or PD98059 until the extraction of the RNA sample.

siRNA

Sequences of siRNAs (Invitrogen, Carlsbad, CA) were as follows: 5′-aactcacctgtgaccaaaaca-3′ for 4EBP1, 5′-aagactccaaagtagaagtaa-3′ for 4EBP2 and 5′-aagctggagtg-caagaactca-3′ for 4EBP3. Before using, the siRNAs were dissolved in RNase-free water, denatured once at 98 °C for 1 min and annealed at 37 °C for 1 h. For electroporation of siRNA, 4×10^5 cells and 0.8 μg siRNA were suspended in 400 μl of OPTI-MEM (Invitrogen, Carlsbad, CA) and pulsed at 250 V and 950 μF using GenePulser (Bio Rad, Hercules, CA) at 4 °C. To evaluate the silencing effects of siRNAs, RT-PCR was performed using One-Step RT-PCR Kit (TaKaRa, Ohtsu, Japan) according to the manufacturer's instruction. Primer sequences used were as follows: 4EBP1, 5′-cggaattcgatgtccgggggcagcagctgc-3′ and 5′-ctgactcgagt-taaatgtccatctcaaactgtg-3′, 4EBP2, 5′-cggaattcatgtcctcgt-cagccggcag-3′ and 5′-ctgactcgagtcagatgtccatctcgaac-3′, 4EBP3, 5′-cggaattcatgtcaacgtccactagctg-3′ and 5′-ctgactc-gagttagatgtccatttcaaattg-3′, GAPDH, 5′-tttctcgagatggg-gaaggtgaaggtcg-3′ and 5′-ccggaattctggagggatctcgctcctg-3′.

Acknowledgments

We wish to thank Dr. Gram (Novartis Pharma, Basel) for providing CGP57380. This work was supported by grants-in-aid for cancer research and by the second-term comprehensive 10-year strategy for cancer control and by the Ministry of Health, Labor, and Welfare, as well as grants-in-aid for scientific research from the Ministry of Education, Culture, Sports, Science, and Technology, grants-in-aid by the Japanese Society for the Promotion of Science (JSPS) and by the Program for Promotion of Fundamental Studies in Health Science of the Organization for Pharmaceutical Safety and Research (OPSR) of Japan. T.M. is a recipient of a JSPS Postdoctoral Fellowship.

References

Aizaki, H., Nagamori, S., Matsuda, M., Kawakami, H., Hashimoto, O., Ishiko, H., Kawada, M., Matsuura, T., Hasumura, S., Matsuura, Y., Suzuki, T., Miyamura, T., 2003. Production and release of infectious hepatitis C virus from human liver cell cultures in the three-dimensional radial-flow bioreactor. Virology 314 (1), 16–25.

Akula, S.M., Ford, P.W., Whitman, A.G., Hamden, K.E., Shelton, J.G., McCubrey, J.A., 2004. Raf promotes human herpesvirus-8 (HHV-8/KSHV) infection. Oncogene 23 (30), 5227–5241.

Ali, N., Siddiqui, A., 1995. Interaction of polypyrimidine tract-binding protein with the 5′ noncoding region of the hepatitis C virus RNA genome and its functional requirement in internal initiation of translation. J. Virol. 69 (10), 6367–6375.

Ali, N., Siddiqui, A., 1997. The La antigen binds 5′ noncoding region of the hepatitis C virus RNA in the context of the initiator AUG codon and stimulates internal ribosome entry site-mediated translation. Proc. Natl. Acad. Sci. U.S.A. 94 (6), 2249–2254.

Barber, S.A., Bruett, L., Douglass, B.R., Herbst, D.S., Zink, M.C., Clements, J.E., 2002. Visna virus-induced activation of MAPK is required for virus replication and correlates with virus-induced neuropathology. J. Virol. 76 (2), 817–828.

Blight, K.J., Kolykhalov, A.A., Rice, C.M., 2000. Efficient initiation of HCV RNA replication in cell culture. Science 290 (5498), 1972–1974.

Choo, Q.L., Kuo, G., Weiner, A.J., Overby, L.R., Bradley, D.W., Houghton, M., 1989. Isolation of a cDNA clone derived from a blood-borne non-A, non-B viral hepatitis genome. Science 244, 359–362.

Cornelis, S., Bruynooghe, Y., Denecker, G., Van Huffel, S., Tinton, S., Beyaert, R., 2000. Identification and characterization of a novel cell cycle-regulated internal ribosome entry site. Mol. Cell 5 (4), 597–605.

de Magalhaes, J.C., Andrade, A.A., Silva, P.N., Sousa, L.P., Ropert, C., Ferreira, P.C., Kroon, E.G., Gazzinelli, R.T., Bonjardim, C.A., 2001. A mitogenic signal triggered at an early stage of vaccinia virus infection: implication of MEK/ERK and protein kinase A in virus multiplication. J. Biol. Chem. 276 (42), 38353–38360.

Forton, D.M., Karayiannis, P., Mahmud, N., Taylor-Robinson, S.D., Thomas, H.C., 2004. Identification of unique hepatitis C virus quasispecies in the central nervous system and comparative analysis of internal translational efficiency of brain, liver, and serum variants. J. Virol. 78 (10), 5170–5183.

Fukaya, K., Asahi, S., Nagamori, S., Sakaguchi, M., Gao, C., Miyazaki, M., Namba, M., 2001. Establishment of a human hepatocyte line (OUMS-29) having CYP 1A1 and 1A2 activities from fetal liver tissue by transfection of SV40 LT. In Vitro Cell. Dev. Biol.: Anim. 37 (5), 266–269.

Gao, X., Ikuta, K., Tajima, M., Sairenji, T., 2001. 12-*O*-tetradecanoylphorbol-13-acetate induces Epstein–Barr virus reactivation via NF-kappaB and AP-1 as regulated by protein kinase C and mitogen-activated protein kinase. Virology 286 (1), 91–99.

Gingras, A.C., Gygi, S.P., Raught, B., Polakiewicz, R.D., Abraham, R.T., Hoekstra, M.F., Aebersold, R., Sonenberg, N., 1999. Regulation of 4E-BP1 phosphorylation: a novel two-step mechanism. Genes Dev. 13 (11), 1422–1437.

Gingras, A.C., Raught, B., Gygi, S.P., Niedzwiecka, A., Miron, M., Burley,

S.K., Polakiewicz, R.D., Wyslouch-Cieszynska, A., Aebersold, R., Sonenberg, N., 2001. Hierarchical phosphorylation of the translation inhibitor 4E-BP1. Genes Dev. 15 (21), 2852–2864.

Goodman, Z.D., Ishak, K.G., 1995. Histology of hepatitis C virus infection. Semin. Liver. Dis. 15, 70–81.

Hahm, B., Kim, Y.K., Kim, J.H., Kim, T.Y., Jang, S.K., 1998. Heterogeneous nuclear ribonucleoprotein L interacts with the 3′ border of the internal ribosomal entry site of hepatitis C virus. J. Virol. 72 (11), 8782–8788.

He, Y., Yan, W., Coito, C., Li, Y., Gale Jr., M., Katze, M.G., 2003. The regulation of hepatitis C virus (HCV) internal ribosome-entry site-mediated translation by HCV replicons and nonstructural proteins. J. Gen. Virol. 84 (Pt. 3), 535–543.

Herbert, T.P, Tee, A.R., Proud, C.G., 2002. The extracellular signal-regulated kinase pathway regulates the phosphorylation of 4E-BP1 at multiple sites. J. Biol. Chem. 277 (13), 11591–11596.

Hirasawa, K., Kim, A., Han, H.S., Han, J., Jun, H.S., Yoon, J.W., 2003. Effect of p38 mitogen-activated protein kinase on the replication of encephalomyocarditis virus. J. Virol. 77 (10), 5649–5656.

Honda, M., Ping, L.H., Rijnbrand, R.C., Amphlett, E., Clarke, B., Rowlands, D., Lemon, S.M., 1996. Structural requirements for initiation of translation by internal ribosome entry within genome-length hepatitis C virus RNA. Virology 222 (1), 31–42.

Honda, M., Kaneko, S., Matsushita, E., Kobayashi, K., Abell, G.A., Lemon, S.M., 2000. Cell cycle regulation of hepatitis C virus internal ribosomal entry site-directed translation. Gastroenterology 118 (1), 152–162.

Ikeda, M., Sugiyama, K., Mizutani, T., Tanaka, T., Tanaka, K., Sekihara, H., Shimotohno, K., Kato, N., 1998. Human hepatocyte clonal cell lines that support persistent replication of hepatitis C virus. Virus Res. 56 (2), 157–167.

Inoue, Y., Miyazaki, M., Tsuji, T., Sakaguchi, M., Fukaya, K., Huh, N.H., Namba, M., 2001. Reactivation of liver-specific gene expression in an immortalized human hepatocyte cell line by introduction of the human HNF4alpha2 gene. Int. J. Mol. Med. 8 (5), 481–487.

Kishine, H., Sugiyama, K., Hijikata, M., Kato, N., Takahashi, H., Noshi, T., Nio, Y., Hosaka, M., Miyanari, Y., Shimotohno, K., 2002. Subgenomic replicon derived from a cell line infected with the hepatitis C virus. Biochem. Biophys. Res. Commun. 293 (3), 993–999.

Knauf, U., Tschopp, C., Gram, H., 2001. Negative regulation of protein translation by mitogen-activated protein kinase-interacting kinases 1 and 2. Mol. Cell. Biol. 21 (16), 5500–5511.

Laporte, J., Bain, C., Maurel, P., Inchauspe, G., Agut, H., Cahour, A., 2003. Differential distribution and internal translation efficiency of hepatitis C virus quasispecies present in dendritic and liver cells. Blood 101 (1), 52–57.

Lerat, H., Shimizu, Y.K., Lemon, S.M., 2000. Cell type-specific enhancement of hepatitis C virus internal ribosome entry site-directed translation due to 5′ nontranslated region substitutions selected during passage of virus in lymphoblastoid cells. J. Virol. 74 (15), 7024–7031.

Lohmann, V., Korner, F., Koch, J., Herian, U., Theilmann, L., Bartenschlager, R., 1999. Replication of subgenomic hepatitis C virus RNAs in a hepatoma cell line. Science 285 (5424), 110–113.

Lott, W.B., Takyar, S.S., Tuppen, J., Crawford, D.H., Harrison, M., Sloots, T.P., Gowans, E.J., 2001. Vitamin B12 and hepatitis C: molecular biology and human pathology. Proc. Natl. Acad. Sci. U.S.A. 98 (9), 4916–4921.

Luo, H., Yanagawa, B., Zhang, J., Luo, Z., Zhang, M., Esfandiarei, M., Carthy, C., Wilson, J.E., Yang, D., McManus, B.M., 2002. Coxsackievirus B3 replication is reduced by inhibition of the extracellular signal-regulated kinase (ERK) signaling pathway. J. Virol. 76 (7), 3365–3373.

Mader, S., Lee, H., Pause, A., Sonenberg, N., 1995. The translation initiation factor eIF-4E binds to a common motif shared by the translation factor eIF-4 gamma and the translational repressors 4E-binding proteins. Mol. Cell. Biol. 15 (9), 4990–4997.

Miyanari, Y., Hijikata, M., Yamaji, M., Hosaka, M., Takahashi, H., Shimotohno, K., 2003. Hepatitis C virus non-structural proteins in the probable membranous compartment function in viral genome replication. J. Biol. Chem. 278 (50), 50301–50308.

Montes, M., Tagieva, N.E., Heveker, N., Nahmias, C., Baleux, F., Trautmann, A., 2000. SDF-1-induced activation of ERK enhances HIV-1 expression. Eur. Cytokine Network 11 (3), 470–477.

Mothe-Satney, I., Yang, D., Fadden, P., Haystead, T.A., Lawrence Jr., J.C., 2000. Multiple mechanisms control phosphorylation of PHAS-I in five (S/T)P sites that govern translational repression. Mol. Cell. Biol. 20 (10), 3558–3567.

Murata, T., Ohshima, T., Yamaji, M., Hosaka, M., Miyanari, Y., Hijikata, M., Shimotohno, K., 2005. Suppression of hepatitis C virus replicon by TGF-beta. Virology 331 (2), 407–417.

Murphy, F.A., Fauquet, C.M., Bishop, D.H.L., Ghabrial, S.A., Jarvis, A.W., Martelli, G.P., Mayo, M.A., Summers, M.D., 1995. Classification and Nomenclature of Viruses: Sixth Report of the Internal Committee on Taxonomy of Viruses. Springer-Verlag, Vienna, Austria, pp. 424–426.

Neddermann, P., Quintavalle, M., Di Pietro, C., Clementi, A., Cerretani, M., Altamura, S., Bartholomew, L., De Francesco, R., 2004. Reduction of hepatitis C virus NS5A hyperphosphorylation by selective inhibition of cellular kinases activates viral RNA replication in cell culture. J. Virol. 78 (23), 13306–13314.

Otto, G.A., Lukavsky, P.J., Lancaster, A.M., Sarnow, P., Puglisi, J.D., 2002. Ribosomal proteins mediate the hepatitis C virus IRES-HeLa 40S interaction. RNA 8 (7), 913–923.

Patel, J., McLeod, L.E., Vries, R.G., Flynn, A., Wang, X., Proud, C.G., 2002. Cellular stresses profoundly inhibit protein synthesis and modulate the states of phosphorylation of multiple translation factors. Eur. J. Biochem. 269 (12), 3076–3085.

Planz, O., Pleschka, S., Ludwig, S., 2001. MEK-specific inhibitor U0126 blocks spread of Borna disease virus in cultured cells. J. Virol. 75 (10), 4871–4877.

Pleschka, S., Wolff, T., Ehrhardt, C., Hobom, G., Planz, O., Rapp, U.R., Ludwig, S., 2001. Influenza virus propagation is impaired by inhibition of the Raf/MEK/ERK signalling cascade. Nat. Cell Biol. 3 (3), 301–305.

Pyronnet, S., Pradayrol, L., Sonenberg, N., 2000. A cell cycle-dependent internal ribosome entry site. Mol. Cell 5 (4), 607–616.

Raught, B., Gingras, A.C., 1999. eIF4E activity is regulated at multiple levels. Int. J. Biochem. Cell Biol. 31 (1), 43–57.

Reed, K.E., Xu, J., Rice, C.M., 1997. Phosphorylation of the hepatitis C virus NS5A protein in vitro and in vivo: properties of the NS5A-associated kinase. J. Virol. 71 (10), 7187–7197.

Robinson, M.J., Cobb, M.H., 1997. Mitogen-activated protein kinase pathways. Curr. Opin. Cell Biol. 9 (2), 180–186.

Rodems, S.M., Spector, D.H., 1998. Extracellular signal-regulated kinase activity is sustained early during human cytomegalovirus infection. J. Virol. 72 (11), 9173–9180.

Scheper, G.C., Proud, C.G., 2002. Does phosphorylation of the cap-binding protein eIF4E play a role in translation initiation? Eur. J. Biochem. 269 (22), 5350–5359.

Sizova, D.V., Kolupaeva, V.G., Pestova, T.V., Shatsky, I.N., Hellen, C.U., 1998. Specific interaction of eukaryotic translation initiation factor 3 with the 5′ nontranslated regions of hepatitis C virus and classical swine fever virus RNAs. J. Virol. 72 (6), 4775–4782.

Subkhankulova, T., Mitchell, S.A., Willis, A.E., 2001. Internal ribosome entry segment-mediated initiation of c-Myc protein synthesis following genotoxic stress. Biochem. J. 359 (Pt. 1), 183–192.

Takahashi, H., Yamaji, M., Hosaka, M., Kishine, H., Hijikata, M., Shimotohno, K., 2005. Analysis of the 5′ end structure of HCV subgenomic RNA replication in an Huh7 cell line. Intervirology 48 (2–3), 104–111.

Tamemoto, H., Kadowaki, T., Tobe, K., Ueki, K., Izumi, T., Chatani, Y., Kohno, M., Kasuga, M., Yazaki, Y., Akanuma, Y., 1992. Biphasic activation of two mitogen-activated protein kinases during the cell cycle in mammalian cells. J. Biol. Chem. 267 (28), 20293–20297.

Tsukiyama-Kohara, K., Iizuka, N., Kohara, M., Nomoto, A., 1992. Internal ribosome entry site within hepatitis C virus RNA. J. Virol. 66 (3), 1476–1483.

Watashi, K., Hijikata, M., Hosaka, M., Yamaji, M., Shimotohno, K., 2003. Cyclosporin A suppresses replication of hepatitis C virus genome in cultured hepatocytes. Hepatology 38 (5), 1282–1288.

Zheng, Y., Li, J., Johnson, D.L., Ou, J.H., 2003. Regulation of hepatitis B virus replication by the ras-mitogen-activated protein kinase signaling pathway. J. Virol. 77 (14), 7707–7712.

Zhu, H., Liu, C., 2003. Interleukin-1 inhibits hepatitis C virus subgenomic RNA replication by activation of extracellular regulated kinase pathway. J. Virol. 77 (9), 5493–5498.

Molecular Cell, Vol. 19, 111–122, July 1, 2005, Copyright ©2005 by Elsevier Inc. DOI 10.1016/j.molcel.2005.05.014

Cyclophilin B Is a Functional Regulator of Hepatitis C Virus RNA Polymerase

Koichi Watashi, Naoto Ishii, Makoto Hijikata, Daisuke Inoue, Takayuki Murata, Yusuke Miyanari, and Kunitada Shimotohno*
Laboratory of Human Tumor Viruses
Department of Viral Oncology
Institute for Virus Research
Kyoto University
Kyoto 606-8507
Japan

Summary

Viruses depend on host-derived factors for their efficient genome replication. Here, we demonstrate that a cellular peptidyl-prolyl *cis-trans* isomerase (PPIase), cyclophilin B (CyPB), is critical for the efficient replication of the hepatitis C virus (HCV) genome. CyPB interacted with the HCV RNA polymerase NS5B to directly stimulate its RNA binding activity. Both the RNA interference (RNAi)-mediated reduction of endogenous CyPB expression and the induced loss of NS5B binding to CyPB decreased the levels of HCV replication. Thus, CyPB functions as a stimulatory regulator of NS5B in HCV replication machinery. This regulation mechanism for viral replication identifies CyPB as a target for antiviral therapeutic strategies.

Introduction

CyP was originally discovered as a cellular factor with high affinity for the immunosuppressant cyclosporin A (CsA) (Handschumacher et al., 1984; Schreiber, 1991). CyPs are a family of PPIases, which catalyze the *cis-trans* interconversion of peptide bonds amino-terminal to proline residues, facilitating changes in protein conformation (Fischer et al., 1998; Takahashi, 1999; Waldmeier et al., 2003). In mammals, CyPs include more than ten subtypes (Braaten and Luban, 2001; Takahashi, 1999; Waldmeier et al., 2003). CyP family members function in numerous cellular processes, including transcriptional regulation, immune response, protein secretion, and mitochondrial function (Braaten and Luban, 2001; Brazin et al., 2002; Colgan et al., 2004; Duina et al., 1996; Rycyzyn and Clevenger, 2002; Waldmeier et al., 2003). In this study, we report the involvement of CyPB in HCV genome replication and propose its molecular mechanism.

HCV is a major causative agent of liver diseases such as chronic hepatitis, liver cirrhosis, and hepatocellular carcinoma (Liang et al., 1993). HCV, a member of the Flaviviridae family, has a positive-strand RNA genome. The genome encodes a large precursor polyprotein, which is cleaved by host and viral proteases to generate at least ten functional viral proteins: core, envelope (E)1, E2, p7, nonstructural protein (NS)2, NS3, NS4A, NS4B, NS5A, and NS5B (Grakoui et al., 1993). NS5B is an RNA-dependent RNA polymerase (RdRp), which is crucial in viral genome replication (Bartenschlager and Lohmann, 2001; Tellinghuisen and Rice, 2002). Until recently, research into HCV genome replication has been hampered by the lack of a cell culture system that can efficiently reproduce HCV infection and proliferation. Even now, we do not have an in vitro system that efficiently produces infectious HCV viral particles. Lohmann et al. previously established the HCV subgenomic replicon system in which the HCV subgenomic RNA autonomously replicates in Huh-7 cells (Lohmann et al., 1999), which we refer to throughout this report as HCV replicon cells. This replicon system enables us to investigate HCV genome replication in a cell culture system. By using this system, several groups have recently reported that HCV genome replication occurs in a distinct, subcellular replication complex (RC), which includes viral genome RNA and HCV proteins (Aizaki et al., 2004; Egger et al., 2002; El-Hage and Luo, 2003; Gosert et al., 2003; Miyanari et al., 2003), in a manner similar to other RNA viruses (Noueiry and Ahlquist, 2003). The RC is formed on intracellular membranes, including the endoplasmic reticulum (ER) membrane. This membrane structure protects the RC from external nucleases and proteases, which seems advantageous for efficient viral genome replication (Aizaki et al., 2004; El-Hage and Luo, 2003; Miyanari et al., 2003). However, the role of cellular factors directly regulating the activity of the RC has remained unclear.

We and other groups have previously reported that CsA has the potential to suppress HCV genome replication (Nakagawa et al., 2004; Watashi et al., 2003a). In this study, we used CsA as a bioprobe to identify cellular factors involved in HCV genome replication. This strategy revealed that CyPB, one of the cellular targets of CsA, was required for the efficient replication of the HCV genome in the cells. Investigation into the molecular mechanism showed that CyPB interacted with NS5B and directly promoted its RNA binding activity. The CyPB-NS5B association is a potent target for the development of an antiviral therapeutics.

Results

Functional Inhibition of CyP Suppressed HCV Genome Replication

As HCV does not efficiently infect cultured cells, we studied viral replication by using HCV replicon cells. We have previously reported that CsA treatment suppressed HCV genome replication (Watashi et al., 2003a). A number of studies have shown that CsA has three major cellular targets: CyP, the calcineurin (CN)-NF-AT pathway, and P-glycoprotein (P-gp) (Loor et al., 2002; Takahashi, 1999) (Figure 1A). We initially determined which of these cellular targets of CsA were involved in HCV genome replication. We examined the effect of several CsA mutants (functional characteristics are shown in Figure 1A) on HCV genome replication by real-time RT-PCR and immunoblot analyses. CsA, (8′-OH-MeBmt[1])Cs,

*Correspondence: kshimoto@virus.kyoto-u.ac.jp

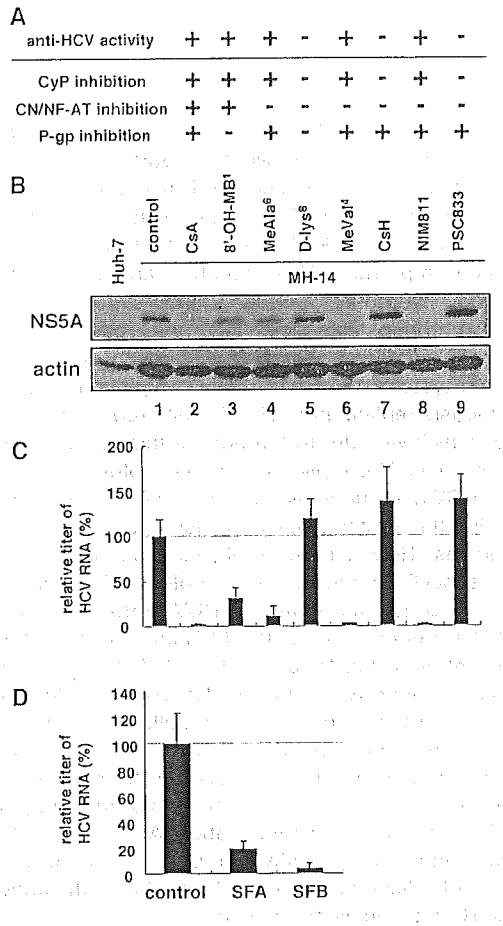

Figure 1. Functional Inhibition of Cyclophilin Suppressed HCV Genome Replication

(A) Characteristic features of cyclosporin A (CsA) and its derivatives, 8'-OH-MeBmt[1]-Cs (8'-OH-MB[1]), MeAla[6]-Cs (MeAla[6]), D-lys[8]-Cs (D-lys[6]), MeVal[4]-Cs (MeVal[4]), cyclosporin H (CsH), NIM811, and PSC833. "Anti-HCV activity" summarizes the potential for each derivative to decrease HCV replication, defined as + (effective), or – (not effective). The inhibition activity to cellular cyclophilin (CyP), calcineurin (CN)-NF-AT pathway, and P-glycoprotein (P-gp) is similarly defined by ±.

(B and C) MH-14 cells, carrying the HCV subgenomic replicon, were treated with 1 μg/ml CsA or its derivatives for seven days. Levels of NS5A (B, top) and actin as an internal control (B, bottom) in these cells were detected by immunoblot analysis. HCV RNA titers were quantified by real-time RT-PCR analysis, and relative titer is shown in (C). The data represent the means of three independent experiments. Error bars represent the SD.

(D) HCV RNA titers in MH-14 cells treated with 3 μg/ml sanglifehrin (SF)A and SFB for seven days were measured as described in (C). Error bars represent the SD.

(MeAla[6])Cs, (MeVal[4])Cs, and NIM811 had anti-HCV activity, decreasing both HCV protein production and HCV RNA titer in HCV replicon cells (Figures 1B and 1C, lanes 2, 3, 4, 6, and 8). In contrast, (D-lys[8])Cs, CsH, and PSC833 had little effect on HCV genome replication (Figures 1B and 1C, lanes 5, 7, and 9). A comparison of anti-HCV activity with the characteristics of these CsA derivatives (Figure 1A) indicates that the anti-HCV activity correlated with inhibition of CyP, but not the CN-NF-AT pathway or P-gp. Sanglifehrin (SF)A and SFB, additional CyP inhibitors (Sanglier et al., 1999), also decreased HCV RNA titers in replicon cells (Figure 1D), suggesting that CyP is linked to HCV genome replication.

CyPB Played a Significant Role in HCV Genome Replication

In mammalian cells, the CyP family contains more than ten subfamilies (Braaten and Luban, 2001; Takahashi, 1999; Waldmeier et al., 2003). CyPA and CyPB are the most abundant subtypes (Waldmeier et al., 2003). We applied RNAi methods to investigate the role of CyPs in HCV genome replication. By introducing small interfering RNA (siRNA) designed to recognize several CyP subtypes (si-CyP[broad]) (see Experimental Procedures), both endogenous CyPA and CyPB proteins, but not actin, were downregulated in replicon cells (Figure 2A, lane 2). The titer of HCV RNA in these cells was diminished to approximately one-fifth of the levels seen in the cells transfected with a randomized siRNA (si-control) (Figure 2B). Specific knockdown of endogenous CyPB also significantly reduced HCV RNA titer, whereas depletion of endogenous CyPA did not (Figure 2A, lanes 3 and 4, and Figure 2B). Depletion of CyPB did not affect cell proliferation (data not shown). A similar result was obtained in another HCV replicon cell clone, 50-1 (Watashi et al., 2003a) (data not shown). Introduction of siRNAs specific for other CyP family members, CyPC, CyPE, or CyPH (Figure 2C), had no effect on HCV RNA titer in replicon cells (Figure 2D). These data suggest that among the CyP family, CyPB is specifically linked to HCV genome replication. Also, in a system in which HCV genome replication can be monitored by luciferase activity (Murata et al., 2005) (Figure 2E), depletion of CyPB inhibited HCV genome replication (Figure 2F). This effect was reversed by the exogenous overproduction of FLAG-tagged CyPB (Figure 2G). These results further indicate that CyPB plays a significant role in HCV genome replication. A weak, nonspecific cross-silencing effect of si-CyPA on CyPB (Figure 2A, lane 3) did not affect HCV RNA titer, suggesting the possibility that the expression level of CyPB has a threshold to support HCV genome replication.

CyPB Interacted with HCV NS5B

To clarify the mechanisms underlying CyPB regulation of HCV genome replication, we analyzed the molecular interaction between CyPB and HCV proteins expressed in HCV replicon cells by GST pull-down. Human immunodeficiency virus (HIV)-1 Gag, which binds CyP family proteins (see Discussion) (Braaten and Luban, 2001; Luban et al., 1993), was used as a positive control (Figure 3A, panel e). As a result, the GST fusion of CyPB (GST-CyPB) coprecipitated only the NS5B viral protein (Figure 3A, panel d). The interaction between NS5B and CyPB was confirmed by immunoprecipitation of NS5B from replicon cells ectopically expressing CyPB (Figure 3B, lane 4). In addition, endogenous CyPB copurified with NS5B from replicon cells (Figure 3C, lane 2). Endogenous CyPB also associated with exogenously expressed NS5B in Huh-7 cells (Figure 3D, lane 4). In contrast, we could not detect the binding of CyPA to NS5B by using either a GST pull-down assay or an immuno-

precipitation assay (Figure 3A, panel d and Figure 3B, lane 8). These results suggest that CyPB specifically interacts with NS5B. CyPBΔPPI, which was previously shown to lose the catalytic activity (Rycyzyn and Clevenger, 2002), had a strong binding to NS5B (Figure 3B, lane 6).

GST pull-down assays demonstrated that the CyPB-NS5B interaction was reduced in a dose-dependent manner after treatment with CsA, which is an inhibitor of HCV genome replication (Figure 3E). Immunoprecipitations demonstrated that CyPB completely dissociated from NS5B in the presence of CsA (Figure 3F, lanes 2 and 4). We then determined the region of the NS5B molecule responsible for binding to CyPB by deletion analysis. The region comprising amino acids (aa) 71–591 of NS5B, which is deficient in RNA binding (Ishii et al., 1999), coprecipitated with GST-CyPB (Figure 3G, panel b). 401–591 and 521–591 aa, but not 201–400 aa, regions could be precipitated with GST-CyPB (Figure 3G, panels c–e). These results indicate that the carboxy (C)-terminal region of NS5B (521–591) interacts with CyPB. On the other hand, aa 1–570, which lack the C-terminal hydrophobic region, had little affinity for GST-CyPB (Figure 3G, panel f). Analysis of additional deletion mutants (Figure 3G, panels g–i) suggests that the whole 521–591 aa region rather than only the C-terminal 21 region (571–591 aa) of NS5B is likely to be important for the interaction with CyPB.

CyPB Associated with NS5B, which Is Functional for HCV Genome Replication

We next examined the subcellular localization of CyPB. In contrast to CyPA, which exhibited a diffuse distribution throughout the cell (Figure 4A, panel a), CyPB concentrated in the perinuclear region (Figure 4A, panel d). CyPB was colocalized with NS5B (Figure 4A, panels c–e), which reportedly resides on the cytoplasmic face of the ER membrane (Schmidt-Mende et al., 2001). To investigate whether CyPB is also located on the cytoplasmic face of the intracellular membrane, we next performed modified immunofluorescence analysis in which we pretreated the cells with digitonin to permeabilize the plasma membrane, but not intracellular membranes, followed by washing out the cytosol (see Experimental Procedures) (Watashi et al., 2001). PDI, a protein in the lumen of the ER, was not detected in this assay (Figure 4B, panel g), whereas CyPB as well as NS5B could be detected around the perinuclear region (Figure 4B, panels i and k). Also in Huh-7 cells, CyPB was observed in the perinuclear region (Figure 4B, panel o). This suggests that a fraction of CyPB is located on the cytoplasmic face of the intracellular membrane (see Discussion).

We labeled the site of newly synthesized HCV RNA by treating the cells with actinomycin D followed by addition of bromouridine (BrU) (El-Hage and Luo, 2003; Gosert et al., 2003; Restrepo-Hartwig and Ahlquist, 1996). In treated replicon cells, labeling was detected in the perinuclear region as previously reported (El-Hage and Luo, 2003; Gosert et al., 2003) (Figure 4A, panel q, shown by green), whereas no signal was observed in Huh-7 cells or replicon cells in the absence of BrU (Figure 4A, panels p and r). This signal merged with the localization of both NS5B and CyPB (Figure 4A, panels g–l).

In cells, a fraction of NS5B is involved in viral genome replication, but another fraction is not (Aizaki et al., 2004; El-Hage and Luo, 2003; Miyanari et al., 2003). These two fractions can be distinguished by digitonin/protease treatment; NS5B that does not function in HCV genome replication is sensitive to digitonin/protease treatment, whereas that participating in the viral RC and functioning for replication is protected from digitonin/protease digestion. After treatment with digitonin/proteinase K followed by washing and permeabilization with Triton X-100 (effective digitonin permeabilization and proteinase K digestion were confirmed by the complete loss of cytoplasmic protein IκBα detection [data not shown]), the signal intensities of NS5B and CyPB staining were reduced. Even under these conditions, a portion of NS5B, CyPB, and BrU was still detected merging in the perinuclear region (Figure 4A, panels m–o, and data not shown), although CyPB in the lumen of the ER could also be detected in this system (the localization of the NS5B-CyPB interaction is discussed further below). By using replicon cells treated with digitonin/proteinase K, NS5B and endogenous CyPB still coprecipitated (data not shown). Moreover, HCV RNA copurified with anti-CyPB as well as anti-NS5B antibody from the replicon cells crosslinked by formaldehyde (Figure 4C), suggesting the association between CyPB and NS5B-HCV RNA complex in the cells. These data cumulatively suggest that CyPB associates with a fraction of NS5B that is functional for viral genome replication.

CyPB Stimulated RNA Binding Activity of NS5B

To investigate which function of NS5B was modulated by CyPB, we first assumed the possibility that CyPB might alter formation of the RC like hVAP-33 does (see Discussion) (Gao et al., 2004). We estimated the amount of HCV proteins in the RC by examining the levels of digitonin/protease-resistant NS5A and NS5B as described previously (Miyanari et al., 2003). The amount of NS5A and NS5B resistant to digitonin/proteinase K digestion, however, was not affected by treatment with CsA, which inactivates CyPB function (Figure 5A). We did not observe any significant effect on the total protein levels of NS5A and NS5B after serial treatment with CsA for up to 24 hr (Figure 5A, lanes 1 and 6; Figure 5B, lower right panels; and Figure 5D, upper panel lanes 1 and 2). CsA treatment also had no effect on the subcellular localization of NS5B (data not shown). The RNA synthesis activity of the isolated RC, however, was significantly reduced after this CsA treatment condition (Figure 5B).

These results raised the possibility that CyPB directly regulated the function of NS5B within the RC. NS5B binds HCV RNA as a template to function as an RdRp. We therefore investigated the effect of CyPB on the RNA binding activity of NS5B in replicon cells by using poly-U Sepharose beads as a model RNA substrate, as described previously (Ishii et al., 1999; Lohmann et al., 1997; Qin et al., 2001). The association of NS5B with poly-U RNA was confirmed by using replicon cells (Fig-

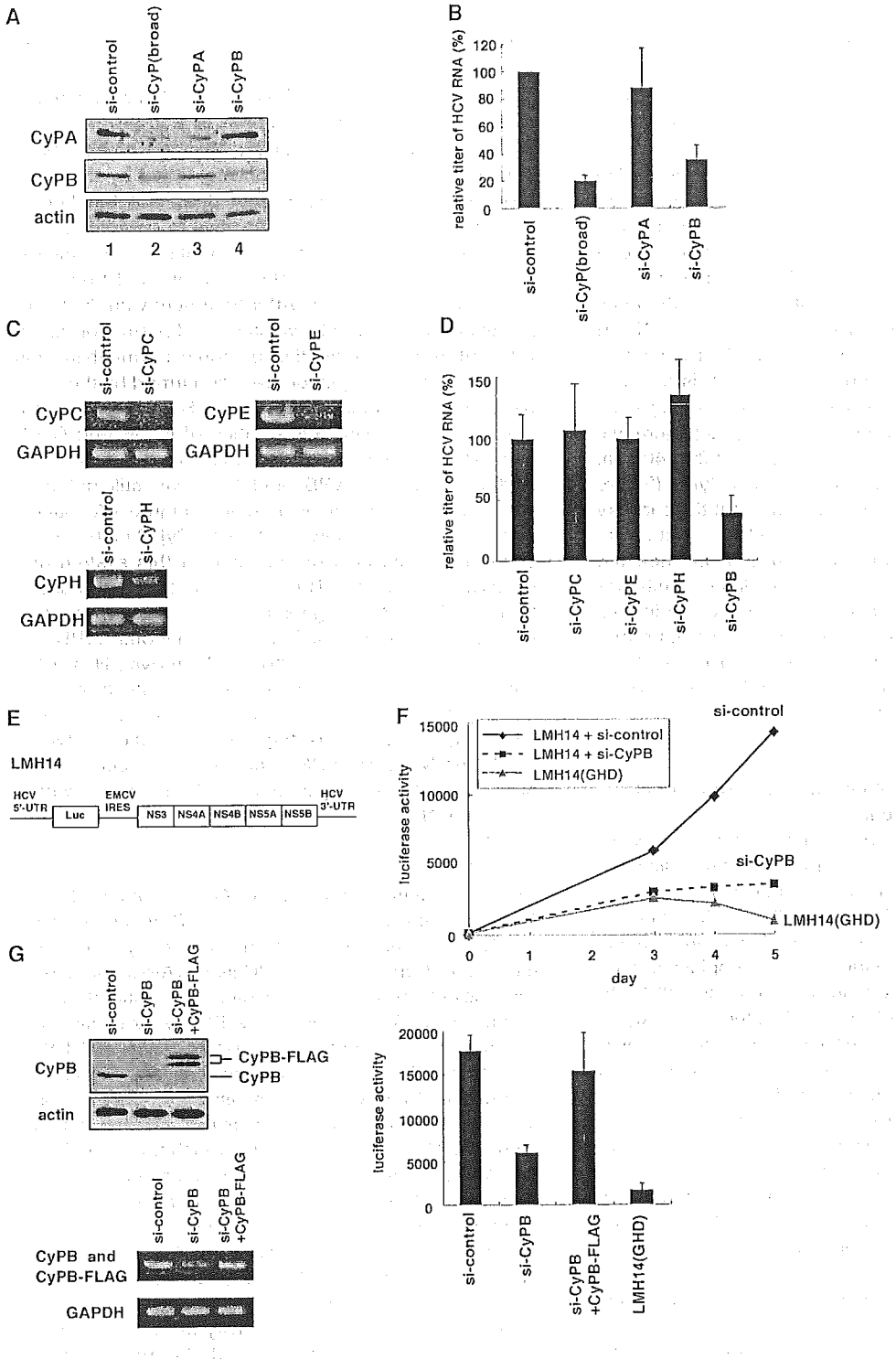

Figure 2. CyPB Regulated HCV Genome Replication

(A) Knockdown of endogenous CyPA and CyPB proteins. MH-14 cells were transfected with siRNA specific for CyPA (si-CyPA), CyPB (si-CyPB), or a broad range of CyP subtypes (si-CyP[broad]) or with a randomized siRNA (si-control). At 72 hr posttransfection, CyPA (top), CyPB (middle), and actin as an internal control (bottom) were detected in total cell lysates by immunoblot analysis.

(B) Depletion of CyPB decreased HCV RNA titers. At 5 days posttransfection of siRNA, HCV RNA titers were quantified by real-time RT-PCR analysis. The data represent the means of three independent experiments. Error bars represent the SD.

(C) siRNA constructs specific for CyPC (si-CyPC), CyPE (si-CyPE), CyPH (si-CyPH), or si-control were introduced into MH-14 cells. At 72 hr posttransfection, we analyzed the mRNA levels of CyPC, CyPE, CyPH, and GAPDH as an internal control by RT-PCR analysis.

(D) The experimental procedure is the same as described in (B). Error bars represent the SD.

(E) Schematic representation of the LMH14 RNA construct, which carries the luciferase gene driven by the HCV 5′-untranslated region (UTR)

ure 5C, upper panel lane 6). Endogenous CyPB, but not CyPA, also coprecipitated with poly-U RNA (Figure 5C, middle and lower panels lane 6). In Huh-7 cells, however, such CyPB-RNA binding was not observed (Figure 5C, lower panel lane 4), suggesting that CyPB binding to RNA is dependent on NS5B. The RNA binding affinity of NS5B isolated from the digitonin/protease-resistant fraction was largely abolished by CsA treatment (Figure 5D, upper panel lane 6), which abrogated the interaction of CyPB with NS5B (Figure 3F, lane 4). A similar result was obtained in another replicon cell clone, 50-1 (data not shown). siRNA-mediated knockdown of the endogenous CyPB also reduced the NS5B-poly-U RNA binding within the digitonin/protease-resistant fraction (Figure 5E, lane 6). These data suggest that CyPB promotes the binding of NS5B to RNA. This effect of CyPB was further documented by using an in vitro RNA binding assay. The binding of NS5B to either poly-U (Figure 5F) or poly-A (data not shown) RNA was increased by the addition of recombinant GST-CyPB. RNA binding, however, was unaffected by the addition of either recombinant GST-CyPA or GST-CyPBΔPPI, a PPIase-inactive point mutant of CyPB (Rycyzyn and Clevenger, 2002) that retained strong binding to NS5B (Figure 3B, lane 6) (Figure 5F). In contrast, CyPB did not augment the RNA binding activity of NS5B(1–570), which had little affinity for CyPB (Figure 3G, panel f) (Figure 5G). The stimulatory effect of CyPB on the RNA binding activity of NS5B was negated by treatment with CsA (Figure 5H). Although the conditions in this in vitro system differ from the cellular environment, these results clearly demonstrate that CyPB can augment RNA binding activity of NS5B even in vitro.

Association of CyPB with NS5B Was Critical for Efficient Replication of HCV Genome

To examine the physiological relevance of the association of CyPB with NS5B in HCV genome replication, we identified a point mutant of NS5B that was unable to bind to CyPB by alanine scanning mutation analysis on the 521–591 aa region of NS5B. In a GST pull-down assay, NS5B(P540A), which bore the replacement of the proline at 540 aa of NS5B by alanine, had little affinity for GST-CyPB (Figure 6A). We confirmed that NS5B(P540A) did not bind CyPB by immunoprecipitation (Figure 6B, lane 6). This P540A mutation decreased the RNA binding activity of NS5B in replicon cells (Figure 6C, lane 6), supporting our conclusion that CyPB plays a stimulatory role in RNA binding of NS5B. Because the P540A mutation may induce the overall conformational change of NS5B protein and destroy its function, we examined the basal function of NS5B(P540A). The levels of protein production and subcellular localization of exogenously produced NS5B(P540A) in Huh-7 cells were, however, similar to those seen in cells with wild-type (wt) NS5B (data not shown). This mutation did not cripple the molecular function of NS5B itself, including RNA polymerase activity and RNA binding activity in vitro (data not shown). The introduction of this point mutation into the NS5B sequence should not destroy the stem-loop RNA structure of the *cis*-acting replication element in the coding region for NS5B, which is present downstream of the P540 codon (Lee et al., 2004; You et al., 2004). The association of NS5B with the ER membrane via its 571–591 aa region is reportedly essential for HCV replication in cells (Moradpour et al., 2004). NS5B(P540A) still associated with intracellular membrane fractions (data not shown). Thus, NS5B(P540A) possessed basal functions of NS5B as far as we examined. However, the replication competency of HCV replicon RNA carrying this one point mutation was significantly decreased from levels observed for the wt in the luciferase assay system (Figure 6D). In this assay, we did not find any reversions at the second site or back to the wt within the NS5B-coding region in HCV replicon RNA of the transfected cells (data not shown). The colony formation assay also demonstrated a reduction in HCV genome replication with the NS5B P540A mutant (Figure 6E). These data suggest that the functional regulation of NS5B by CyPB is critical for the efficient replication of the HCV genome in the cells.

Discussion

Viruses exploit cellular factors for their efficient proliferation. Although it was recently reported that a SNARE-like protein, hVAP-33, augmented HCV replication by modulating RC formation (Gao et al., 2004), cellular factors directly regulating the activity of the RC have remained unknown. By using CsA, a compound exerting a strong anti-HCV potential, we determined that CyPB is required for efficient replication of the HCV genome. This cellular factor regulates HCV genome replication through modulation of the RNA binding activity of NS5B. CsA impaired this regulation of NS5B-RNA binding by CyPB to inhibit HCV genome replication. Previously, the CyP family was known to regulate the function of specific substrates such as calcineurin (Schreiber, 1992), prolactin (Rycyzyn and Clevenger, 2002), Itk (Brazin et al., 2002; Colgan et al., 2004), adenine nucleotide translocase (Waldmeier et al., 2003), and steroid receptors (Duina et al., 1996) by altering

and the coding region for HCV NS3 to NS5B whose expression is regulated by the EMCV IRES. By using this RNA construct, HCV replication can be monitored by measuring resultant luciferase activity as described previously (Murata et al., 2005).

(F) Suppression of HCV replication after CyPB knockdown. Cured MH-14 cells were transfected with LMH14 or LMH14(GHD) RNA together with si-control or si-CyPB. After 3, 4, or 5 days, luciferase activities were measured to plot against the time course. Solid line, transfected with LMH14 RNA and si-control; broken line, LMH14 RNA and si-CyPB; and faint line, LMH14(GHD) RNA, a replication-deficient mutant of LMH14 used as a negative control.

(G) On the right, cured MH-14 cells were transfected with LMH14 RNA plus si-control (si-control), LMH14 RNA plus si-CyPB (si-CyPB), LMH14 RNA plus si-CyPB and the expression plasmid for FLAG-tagged CyPB (si-CyPB + CyPB-FLAG), or LMH14(GHD) RNA (LMH14[GHD]). Luciferase activities were then quantified at 5 days posttransfection. Error bars represent the SD. Left panels show the immunoblot analysis (upper panels) by using anti-CyPB and anti-actin antibody and RT-PCR analysis (lower panels) by using the primer detecting CyPB and GAPDH upon the transfection of si-control, si-CyPB, and si-CyPB with CyPB-FLAG.

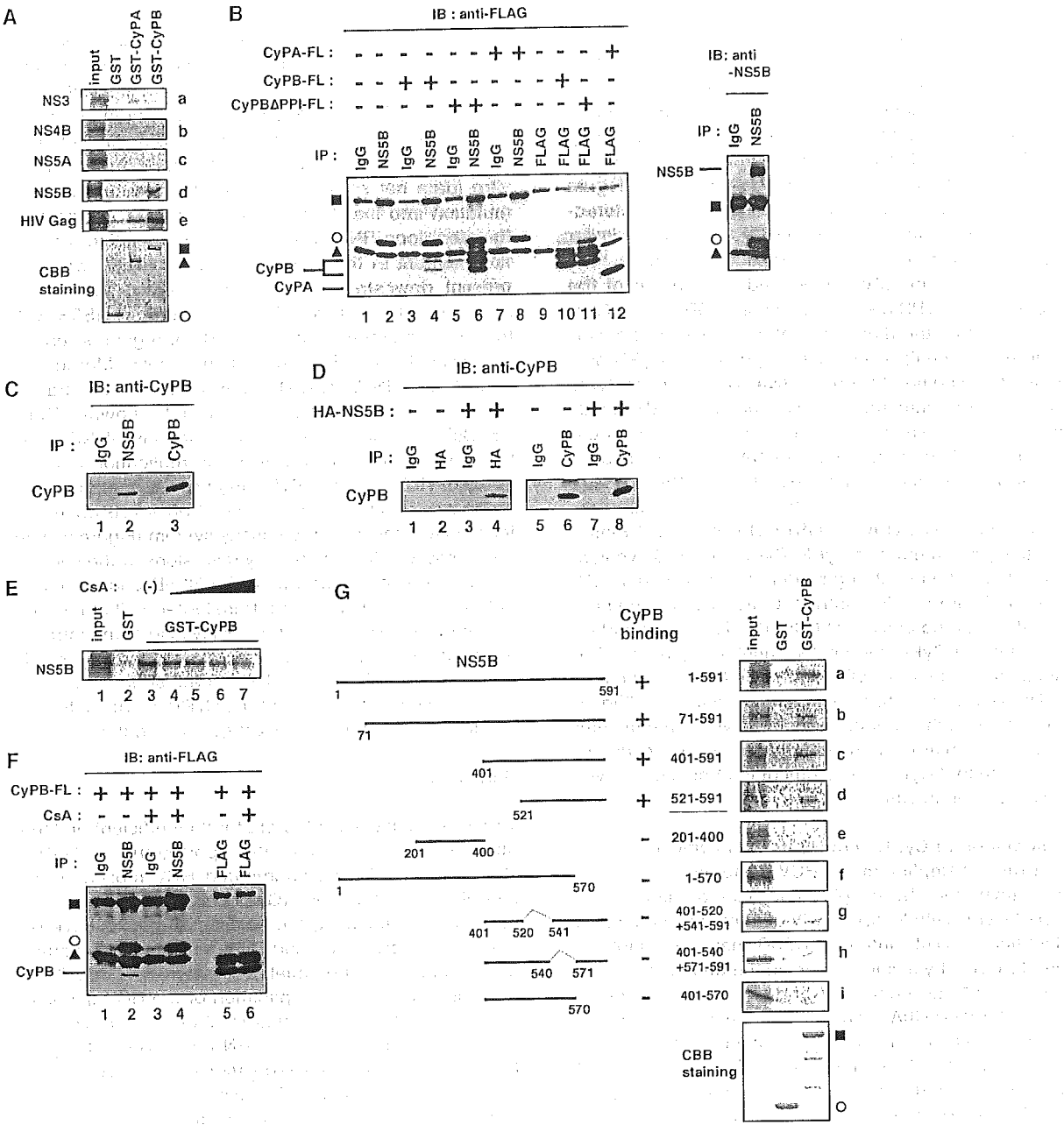

Figure 3. CyPB Interacted with HCV NS5B

(A) [^{35}S]-labeled in vitro translation products of HCV NS3 (panel a), NS4B (panel b), NS5A (panel c), NS5B (panel d), and HIV-1 Gag as a positive control (panel e) were incubated with recombinant GST fusions of CyPA or CyPB (GST-CyPA or GST-CyPB, respectively) or with GST as a negative control. "Input" designated the signal for 1/10 of the amount of [^{35}S]-labeled product used in the pull-down assay. CBB staining patterns for the pulled-down proteins are shown in the bottom panel. Open circle, GST; closed triangle, GST-CyPA; and closed square, GST-CyPB.

(B) Coimmunoprecipitation from lysates of MH-14 cells transfected with expression plasmids for FLAG-tagged CyPA (CyPA-FL) (lanes 7, 8, and 12), CyPB (CyPB-FL) (lanes 3, 4, and 10), CyPBΔPPI (CyPBΔPPI-FL) (lanes 5, 6, and 11), or empty vector (lanes 1, 2, and 9 and right panel). The plasmids used for transfection are indicated at the top of the panel by + or −. "IP" designates the antibodies used for immunoprecipitation. Coimmunoprecipitated proteins were detected by immunoblot analysis using either anti-FLAG (left) or anti-NS5B (right) antibodies, respectively. Closed square, Ig heavy chain; closed triangle, Ig light chain; and open circle, nonspecific band. CyPA, CyPB or CyPBΔPPI, and NS5B are indicated. Ectopically expressed CyPB showed a double band, consistent with the previous report (Price et al., 1994). The upper-slight band of CyPBΔPPI in lane 5 is likely to show nonspecific binding, because it was not precipitated with IgG in a buffer containing higher concentration of NP-40 (1% NP-40) (data not shown).

(C) Coimmunoprecipitation of endogenous CyPB with NS5B in MH-14 cells. The data are presented as in (B). The immunoprecipitates were detected with an anti-CyPB antibody.

(D) Coimmunoprecipitation of endogenous CyPB with exogenous NS5B in Huh-7 cells. Huh-7 cells were transfected with an expression

protein-protein interactions, nuclear import, enzymatic activity, or protein phosphorylation. In this study, we demonstrated that CyPB also modulated the activity of RNA-protein binding. This information will significantly impact our understanding of the molecular functions of CyP.

Regarding the role of CyP in virus proliferation, CyPA has been reported to be involved in the life cycle of HIV-1. CyPA binds HIV-1 Gag (Luban et al., 1993) and is incorporated into viral particles (Franke et al., 1994; Thali et al., 1994). This CyPA promotes viral infectivity (Braaten and Luban, 2001; Towers et al., 2003). HIV-1 Gag, however, binds to not only CyPA but also most other members of the CyP family (Braaten and Luban, 2001; Luban et al., 1993). In contrast to HIV-1 Gag, HCV NS5B bound CyPB, but not CyPA. Among the CyP family members examined, only CyPB regulated HCV genome replication. The subcellular localization of each CyP subtype varies; CyPA is found in the cytoplasm and nucleus, CyPD in the mitochondria, and CyPE in the nucleus (Takahashi, 1999). CyPB is located mainly in the lumen of the ER (Price et al., 1994; Takahashi, 1999). A subset of CyPB, however, was speculated to localize in the cytoplasm or in ER substructures on the cytoplasmic side (Bram et al., 1993). We found that a portion of CyPB localized on the cytoplasmic face of the ER irrespective of the presence of HCV replicon (Figure 4B), consistent with this previous speculation.

Almost all HCV proteins and genomic RNA are located around the ER (Bartenschlager and Lohmann, 2001). The majority of events in the HCV life cycle, including genome replication, protein maturation, assembly, and budding, occur around intracellular ER-like membranes (Bartenschlager and Lohmann, 2001). NS5B mainly localizes on the cytoplasmic side of the ER membrane through its C-terminal 571–591 aa hydrophobic region (Schmidt-Mende et al., 2001). A subset of the total NS5B participates in the RC, which is thought to have a cytoplasmic side membrane topology and is surrounded by a membrane structure (Aizaki et al., 2004). We cannot conclude clearly where CyPB-NS5B-RNA association occurs. The 521–591 aa region of NS5B, which is the binding region for CyPB, however, is thought to be inserted in the ER lipid bilayer membrane on the cytoplasmic face (Schmidt-Mende et al., 2001). A part of CyPB was also found on the cytoplasmic face of the membranes as described above. Moreover, crosslinking analysis (Figure 4C) suggests the interaction of CyPB with the HCV RNA-NS5B complex, which is likely to occur mainly in the RC. Thus, CyPB likely interacts with NS5B on the cytoplasmic face within the RC compartment (and in the lipid bilayer membrane).

Viral polymerases are promising targets for the development of antiviral agents. Several chemicals targeting NS5B have anti-HCV activity (Wu and Hong, 2003). These compounds directly inhibit the activity of recombinant NS5B in vitro. In addition to these typical anti-HCV compounds, inhibition of the association of CyPB with NS5B may serve as a strategy for the design of antiviral therapeutics. Our findings not only reveal one of the mechanisms of viral replication in the cells but also may lead to the development of antiviral therapeutics.

Experimental Procedures

Cell Culture and Transfection

Huh-7 and cured MH-14 cells (Murata et al., 2005) were cultured in Dulbecco's modified Eagle medium (DMEM) (Invitrogen) supplemented with 10% fetal bovine serum, L-glutanime (Invitrogen), MEM nonessential amino acids (Invitrogen), and kanamycin (Meiji). MH-14 cells, carrying HCV subgenomic replicon (Miyanari et al., 2003), were cultured in the same medium supplemented with 300 μg/ml G418 (Invitrogen). Plasmid transfection was performed as described previously (Watashi et al., 2003b). RNA transfection for the reporter assay was achieved by using DMrie-C transfection reagent (Invitrogen) as recommended by the manufacturer. siRNA was transfected by using siLentFect (BIORAD) according to the manufacturer's protocol.

Reagents

CsA was purchased from Sigma. The CsA derivatives 8′-OH-MeBmt^{1}-Cs, MeAla^{6}-Cs, D-lys^{8}-Cs, MeVal^{4}-Cs, cyclosporin H, NIM811, and PSC833 and the macrolide type CyP inhibitors sanglifehrin A and B were kindly provided by Novartis (Basel, Switzerland). The characteristic feature of each CsA derivative is shown in Figure 1A (for details, see Billich et al. [1995], Loor et al. [2002], and Silverman et al. [1997]). (D-lys^{8})Cs binds CyP in vitro. In cells, however, the effective binding affinity to CyP is low because of inefficient cellular uptake (Billich et al., 1995).

Immunoblot Analysis

Immunoblot analysis was performed essentially as described previously (Watashi et al., 2003b).

Antibodies

The antibodies used in this experiment were anti-NS5A (a generous gift from Dr. Takamizawa, Osaka University), anti-NS5B (10 and 14; kindly provided by Dr. Kohara, Tokyo Metropolitan Institute of Medical Science), anti-actin (Sigma), anti-CyPA (Upstate Cell Signaling), anti-CyPB (Affinity BioReagents), anti-FLAG (M2; Sigma), anti-HA (3F10; Roche), anti-BrdU (Sigma), anti-IκBα (Santa Cruz), anti-PDI (StressGen), and anti-calnexin (StressGen) antibodies.

Real-Time RT-PCR Analysis

Real-time RT-PCR analysis was performed as described previously (Watashi et al., 2003a).

RNAi Technique

siRNA duplexes (si-CyPA, 5′-AAGCATACGGGTCCTGGCATC-3′; si-CyPB, 5′-AAGGTGGAGAGCACCAAGACA-3′; and si-CyP(broad), 5′-AAGCATGTGGTGTTTGGCAAA-3′) containing 3′dTdT over-

plasmid for HA-tagged NS5B (lanes 3, 4, 7, and 8) or an empty vector (lanes 1, 2, 5, and 6). The immunoprecipitates were detected by an anti-CyPB antibody.

(E and F) The interaction of CyPB with NS5B was disrupted by CsA treatment. In (E), a GST pull-down assay between GST-CyPB and NS5B was performed in the absence (lane 3) or presence (lanes 4–7) of CsA. The concentrations of CsA in lanes 4–7 are 0.8, 4, 8, and 16 μg/ml, respectively. In (F), coimmunoprecipitation between CyPB-FL and NS5B in MH-14 cells treated without (lanes 1, 2, and 5) or with 3 μg/ml CsA (lanes 3, 4, and 6) was analyzed.

(G) Mapping of the regions of NS5B responsible for the interaction with CyPB. At the left of the panel, schematic representation of the full-length and truncated mutants of NS5B is shown. The numbers indicate the amino acids residue numbers in NS5B. "CyPB binding" summarizes the results of a GST pull-down assay by ±; GST pull-down data are presented as described in (A).

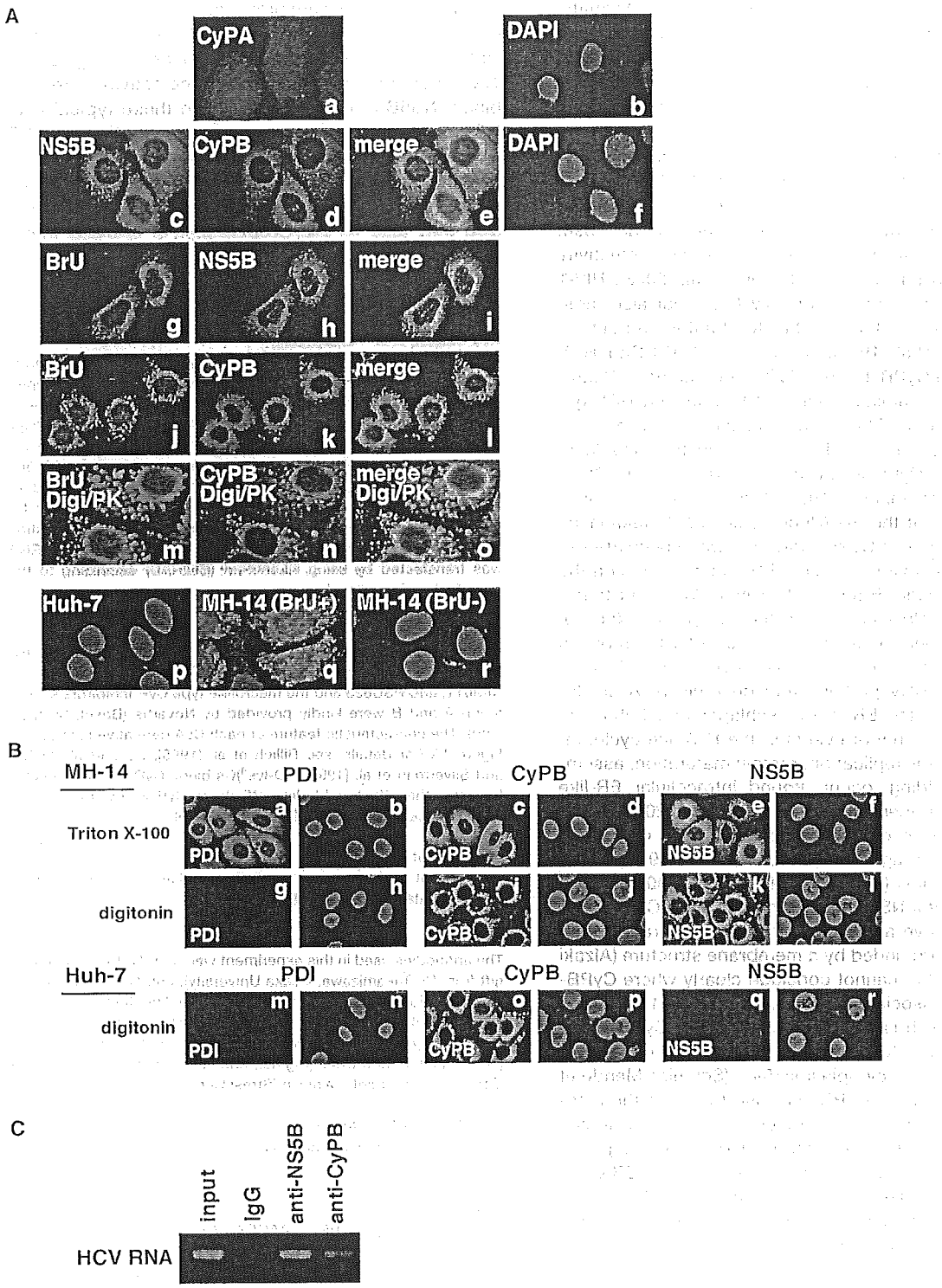

Figure 4. Colocalization of CyPB with NS5B around the Endoplasmic Reticulum

(A) CyPB colocalized with NS5B. Indirect immunofluorescence analysis was performed on MH-14 cells incubated in the absence (panels a–f and r) or presence of actinomycin D/BrU (panels g–o and q). Huh-7 cells were treated with actinomycin D/BrU as a negative control (panel p). Prior to immunofluorescence analysis with permeabilization by Triton X-100, cells were treated with digitonin (Digi) followed by digestion with 0.3 μg/ml proteinase K (PK) in panels m–o. The primary antibodies used were anti-CyPA (panel a, red), anti-CyPB (panels d, k, and n, red), anti-NS5B (panel c, green and panel h, red), and anti-BrdU (panels g, j, m, and p–r, green) antibodies. DAPI was used to visualize the nuclei (panels b, f, and p–r, blue). Panels a–b, c–f, g–i, j–l, and m–o show the same cells. Merged images of green and red signals are shown in panels e, i, l, and o. Panels p–r are the merged images of green (BrU) and blue (DAPI) signals.

(B) A portion of CyPB was located on the cytoplasmic face of the intracellular membrane. MH-14 cells were fixed and followed by permeabili-

hanging sequences were synthesized (QIAGEN). A control nucleotide, si-control, was purchased from Dharmacon (nonspecific control duplex IX). si-CyPC, si-CyPE, and si-CyPH were obtained from Ambion (predesigned siRNA). The sequence of si-CyP(broad) matches 100% with CyPA and CyPB mRNAs, a 20 bp match with CyPH, a 19 bp match with CyPC and CyP40, and a 17 bp match with CyP33. The sequence of si-CyPA and si-CyPB does not have significant identity to mRNA for CyPB and CyPA, respectively.

RT-PCR Analysis

RT-PCR analysis was performed as described (Watashi et al., 2003b) by using the following primer sets: 5′-GTTGGATCCATG GGCCCGGGTC-3′ and 5′-GTTCTCGAGTCACCAATCAGCGATC-3′ for the detection of CyPC, 5′-GTTGAATTCATGGCCACCACCAAG-3′ and 5′-GTTCTCGAGTCACACGTACTCCCCAC-3′ for CyPE, and 5′-GTTGGATCCATGGCGGTGGCAAATTC-3′ and 5′-GTTCTCGAG CTACATCTCCCCACAC-3′ for CyPH.

Luciferase Assay

A luciferase assay monitoring HCV replication levels was performed as previously described (Murata et al., 2005). The reporter RNAs used in this study were LMH14, LMH14(GHD), in which the GDD polymerase motif of NS5B was replaced by GHD to lose replication activity, and LMH14(P540A), in which the proline at position 540 of NS5B was replaced by alanine.

Plasmid Constructs

The CyPA and CyPB cDNAs were obtained by RT-PCR from a human liver cDNA library (Clontech) template by using the following primers: 5′-GTTGGATCCGCCATGGTCAACCCCACCG-3′ and 5′-GTT GAATTCTTCGAGTTGTCCACAGTC-3′ for CyPA and 5′-GTTGGA TCCGCCATGCTGCGCCTCTCC-3′ and 5′-GTTGAATTCCTCCTTG GCGATGGCAA-3′ for CyPB. pGEX-CyPA and pGEX-CyPB, which encode glutathione S-transferase (GST) fusions of CyPA and CyPB were constructed by insertion of the BamHI-EcoRI fragments into the appropriate site of the pGEX-6P1 vector (Clontech). The pCMV-CyPA-FL and pCMV-CyPB-FL plasmids expressing FLAG-tagged CyPA and CyPB, respectively, were obtained by inserting the CyPA and CyPB fragments into the BamHI-EcoRI site of the pCMV-FLAG(C) vector. CyPBΔPPI, of which arginine and phenylalanine at position 95 and 100 of CyPB were replaced by alanines, was an enzymatic-inactive mutant of CyPB (Rycyzyn and Clevenger, 2002). The subcloning of pCMV-CyPBΔPPI-FL, which encodes a FLAG-tagged CyPBΔPPI, was performed essentially as described (Rycyzyn and Clevenger, 2002). Expression plasmids for HCV NS3, NS4B, NS5A, and NS5B (pcDNA-NS3, pcDNA-NS4B, pcDNA-NS5A, and pcDNA-NS5B, respectively) were generated by insertion of PCR-amplified fragments encoding each HCV protein into the pcDNA3 vector (Invitrogen). The series of plasmids expressing deletion mutants of NS5B were constructed by inserting into the pcDNA3 vector various fragments amplified by PCR using appropriate synthetic oligonucleotides as primers and pLMH14 as a template. The primers for oligonucleotide-directed mutagenesis used to generate the NS5B(P540A) mutant were 5′-ACTCCAATTGCGG CTGCGTCC-3′ and 5′-GGACGCAGCCGCAATTGGAGT-3′. LMH14 and LMH14(GHD) have been described previously (Murata et al., 2005). The expression plasmid for HIV-1 Gag was kindly provided by Dr. Adachi, Institute of Health Biosciences, The University of Tokushima.

GST Pull-Down Assay

A GST pull-down assay was performed as described previously (Watashi et al., 2003b).

Immunoprecipitation Assay and RNA-Protein Binding Precipitation Assay

An immunoprecipitation assay was essentially performed as described (Watashi et al., 2003b). For the RNA-protein binding precipitation assay, either cells or digitonin/protease-treated cells were lysed in IP buffer containing 50 mM Tris-HCl (pH 8.0), 150 mM NaCl, 0.5% NP-40, and 1 mM PMSF. After centrifugation, supernatants were incubated for 2 hr with poly-U or protein G Sepharose resin as a negative control (Amersham Biosciences). After four washes with IP buffer, precipitates were analyzed by immunoblot analysis.

Indirect Immunofluorescence Analysis

The normal indirect immunofluorescence analysis in Figures 4A and 4B, panels a–f, was performed as described previously (Watashi et al., 2003b). Briefly, the cells were fixed, and permeabilization with 0.1% Triton X-100 followed. These cells were subjected to the antibody reaction to detect each protein. In Figure 4A, panels g–r, de novo-synthesized HCV RNA was labeled with 5-BrU. Cells were treated with 10 μg/ml actinomycin D to block RNA transcription by cellular DNA-dependent RNA polymerases (Restrepo-Hartwig and Ahlquist, 1996). After a 30 min incubation, 40 mM BrU was added to the culture medium for labeling RNA (Fuchsova et al., 2002). After an additional 2 hr, the cells were subjected to immunofluorescence analysis. In the modified immunofluorescence analysis (Watashi et al., 2001) in Figure 4B, panels g–r, we treated the cells with 50 μg/ml digitonin at 27°C for 5 min to permeabilize the plasma membrane, but not the intracellular membrane. After washing out the cytosol, these cells were fixed and subjected to the antibody reaction.

Crosslinking Assay for the Detection of RNA-Protein Complex

Crosslinking and the subsequent immunoprecipitation were essentially performed as described (Watashi et al., 2003b). The immunoprecipitation was done in the presence of RNase inhibitor and polydI-dC. Recovered immunocomplexes were digested with proteinase K and treated with phenol/chloroform. RT-PCR was performed with the extracted RNA and 5′-TCCCGGTTGGACTTGTCC-3′ and 5′-GCCTATTGGCCTGGAGTG-3′ as a template and primer sets, respectively, by using a one-step RNA PCR kit.

Cell Permeabilization with Digitonin Followed by Digestion with Protease

Digitonin/protease treatment was performed as described previously (Miyanari et al., 2003). Briefly, cells were permeabilized by a 5 min incubation in buffer B containing 50 μg/ml digitonin at 27°C. After two washes in buffer B, cells were treated for 5 min with varying concentrations of proteinase K at 37°C.

RNA Synthesis with the Replication Complex

RNA synthesis reaction was performed as described (Miyanari et al., 2003), using reaction times of 0.5, 1, 2, 4, 6, 12, and 24 hr.

In Vitro RNA Binding Assay

An in vitro RNA binding assay was performed by using poly-U or poly-A Sepharose as a model RNA substrate, as described previously (Ishii et al., 1999). In vitro-translated [^{35}S]-labeled products and poly-U, poly-A, or protein G Sepharose resin as a negative

---

zation with 0.1% Triton X-100 to detect PDI (panel a), CyPB (panel c), and NS5B (panel e) by normal immunofluorescence analysis as a control experiment (Triton X-100). In panels g–r (digitonin), MH-14 (panels g–l) and Huh-7 cells (panels m–r) were permeabilized with 50 μg/ml digitonin followed by extensive washes. These cells were then fixed and subjected to detection of PDI (panels g and m), CyPB (panels i and o), and NS5B (panels k and q). DAPI (panels b, d, f, h, j, l, n, p, and r) shows the nuclear staining in the same cells as that shown in panels a, c, e, g, i, k, m, o, and q.

(C) CyPB associated with HCV RNA-NS5B complex in the cells. Formaldehyde-crosslinked RNA-protein complexes in MH-14 cells were immunoprecipitated with anti-NS5B, anti-CyPB, or normal rabbit IgG (IgG). The RNA extracted from the immunoprecipitates was amplified by RT-PCR as described in the Experimental Procedures. "Input" designated the signal for 1/50 of the amount of cell lysate used in the immunoprecipitation assay.

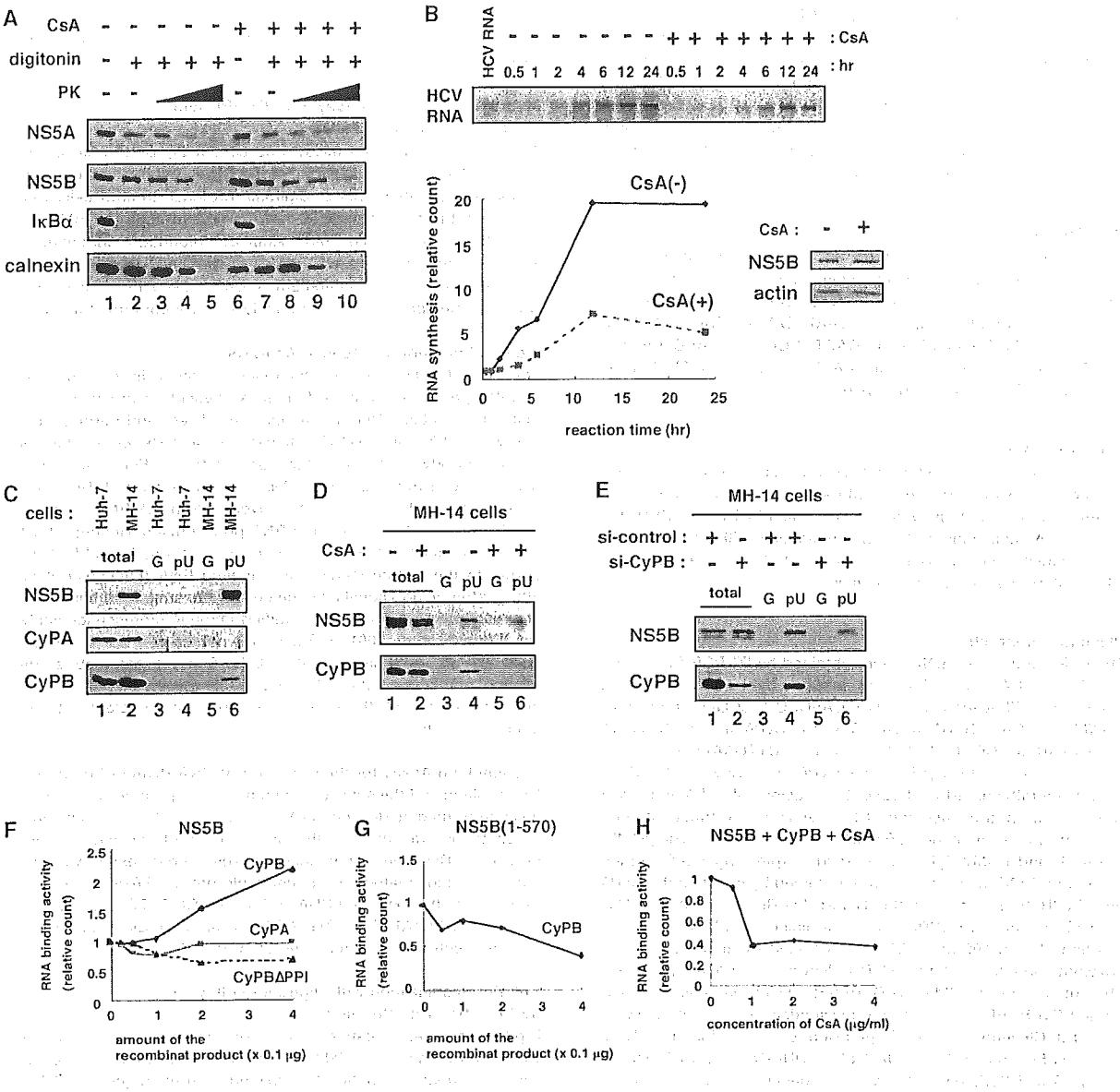

Figure 5. CyPB Stimulated RNA Binding Activity of NS5B

(A) Quantitation of the amount of HCV proteins in the digitonin/protease-resistant fraction. MH-14 cells were treated without (lanes 1–5) or with (lanes 6–10) 3 μg/ml CsA for 24 hr. Cells were then treated without (lanes 1 and 6) or with 50 μg/ml digitonin, followed by digestion with varying concentrations of PK (0 μg/ml for lanes 1, 2, 6, and 7, 0.03 μg/ml for lanes 3 and 8, 0.1 μg/ml for lanes 4 and 9, and 0.3 μg/ml for lanes 5 and 10). NS5A, NS5B, IκBα, and calnexin in whole-cell lysate were detected by immunoblot analysis.

(B) RNA synthesis activity in the HCV RC. MH-14 cells were treated without or with 3 μg/ml CsA for 24 hr. After isolating the RC by digitonin permeabilization, RNA synthesis reaction was performed with varying reaction times (0.5, 1, 2, 4, 6, 12, and 24 hr). At the top of the panel, treatment of CsA and reaction time is summarized. "HCV RNA" indicates the in vitro-synthesized HCV subgenomic replicon RNA. In the lower left panel, the radioactivity of synthesized RNA is plotted against the reaction time. The lower right panels show the protein expression levels of NS5B and actin.

(C) An RNA-protein binding precipitation assay was performed by using Huh-7 or MH-14 cells as described in the Experimental Procedures. The resultant precipitates were detected by immunoblot analysis with anti-NS5B (top), anti-CyPA (middle), and anti-CyPB (bottom) antibodies. "Total" indicates 1/6 of the amount of cell lysate used in the precipitation assay. "G" and "pU" designate the samples using protein G Sepharose and poly-U Sepharose as a resin, respectively.

(D) MH-14 cells treated with digitonin followed by digestion in 0.5 μg/ml PK were used for an RNA-protein binding precipitation assay with anti-NS5B antibody (top). Prior to the assay, CsA was treated (lanes 2, 5, and 6) or left untreated (lanes 1, 3, and 4) for 24 hr. CyPB levels were also examined in CsA-treated or untreated cells (bottom).

(E) MH-14 cells were transfected with si-control or si-CyPB. After 72 hr, cells were treated with digitonin/PK and analyzed as in (C).

(F–H) An in vitro binding assay was performed as described in the Experimental Procedures. [^{35}S]-labeled in vitro translation products of either the full-length NS5B (F and H) or the 1–570 aa region of NS5B (G) were incubated with poly-U Sepharose in the presence of either recombinant GST-CyPB (F–H), GST-CyPA (F), or GST-CyPBΔPPI (F). In (H), varying concentrations of CsA were also added to the reaction mixtures. The radioactivity of NS5B protein in the pulled-down fraction was counted to plot against either the amount of the recombinant product (F and G) or the concentration of CsA (H). In (F), the solid line represents being in the presence of GST-CyPB; the broken line, GST-CyPBΔPPI; and the faint line, GST-CyPA. These results were reproduced in three independent experiments.

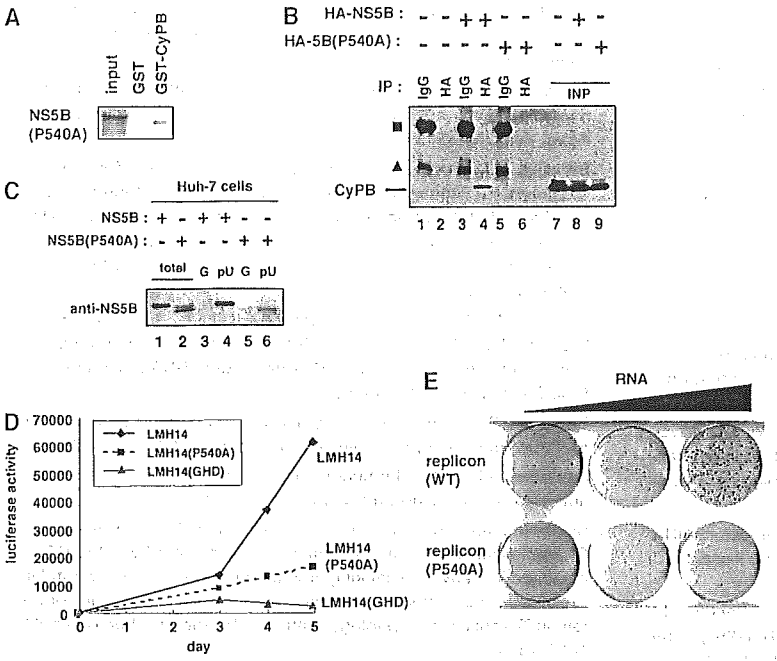

Figure 6. Association of CyPB with NS5B Was Critical for the Efficient Replication of the HCV Genome

(A) A GST pull-down assay was performed and presented as described in Figure 3A.

(B) An immunoprecipitation assay was performed as described in Figure 3B. The expression plasmid for HA-tagged NS5B (lanes 3, 4, and 8) and NS5B(P540A) (lanes 5, 6, and 9) and empty vector (lanes 1, 2, and 7) was used for the transfection. "INP" indicates 1/6 of the amount of cell lysate used for the immunoprecipitation.

(C) An RNA-protein binding precipitation assay was performed by using Huh-7 cells transfected with the expression vector for NS5B (lanes 1, 3, and 4) or NS5B(P540A) (lanes 2, 5, and 6) as described in Figure 5C.

(D) Luciferase assays were performed and are presented as in Figure 2F. Solid line, LMH14; broken line, LMH14(P540A); and faint line, LMH14(GHD).

(E) Colony formation assay. The subgenomic replicon RNA (replicon[wt]) and a replicon RNA carrying the P540A mutation in NS5B (replicon[P540A]) at various amount (2.5 μg in the left wells, 5 μg in the center wells, and 10 μg in the right wells) was transfected into Huh-7 cells. The colony formation assay was performed as described in the Experimental Procedures.

control were incubated in the presence of a varying amount of GST-fusion proteins, including GST-CyPB, GST-CyPA, and GST-CyPBΔPPI, at 4°C for 1–12 hr. In Figure 5H, CsA was added simultaneously. After five washes, resin bound radiolabeled proteins were fractionated, and its radioactivity was quantitated.

Colony Formation Assay

Plasmids were linearized with XbaI and transcribed into RNA in vitro by using a MEGAscript T7 kit (Ambion) according to the manufacturer's protocol. In vitro-transcribed RNA (2.5–10 μg) was transfected into Huh-7 cells by using DMrie-C transfection reagent. At 48 hr posttransfection, 1 mg/ml G418 was added to the medium. ~3 weeks later, cells were fixed and stained with crystal violet.

Acknowledgments

We are grateful to Dr. Takamizawa at Osaka University for an anti-NS5A antibody, Dr. Kohara at Tokyo Metropolitan Institute of Medical Science for an anti-NS5B antibody, and Dr. Adachi at the Institute of Health Biosciences, the University of Tokushima for an expression plasmid for HIV-1 Gag. We also appreciate Novartis (Basel, Switzerland) for providing CsA derivatives and sanglifehrins. This work was supported by grants in aid for cancer research and for the second-term comprehensive 10 year strategy for cancer control from the Ministry of Health, Labor, and Welfare; through grants in aid for scientific research from the Ministry of Education, Culture, Sports, Science and Technology; by grants in aid for Research for the Future from the Japanese Society for the Promotion of Science; and by the Program for Promotion of Fundamental Studies in Health Science of the Organization for Pharmaceutical Safety and Research (OPSR) of Japan.

Received: February 9, 2005
Revised: April 13, 2005
Accepted: May 18, 2005
Published: June 30, 2005

References

Aizaki, H., Lee, K.J., Sung, V.M., Ishiko, H., and Lai, M.M. (2004). Characterization of the hepatitis C virus RNA replication complex associated with lipid rafts. Virology *324*, 450–461.

Bartenschlager, R., and Lohmann, V. (2001). Novel cell culture systems for the hepatitis C virus. Antiviral Res. *52*, 1–17.

Billich, A., Hammerschmid, F., Peichl, P., Wenger, R., Zenke, G., Quesniaux, V., and Rosenwirth, B. (1995). Mode of action of SDZ NIM *811*, a nonimmunosuppressive cyclosporin A analog with activity against human immunodeficiency virus (HIV) type 1: interference with HIV protein-cyclophilin A interactions. J. Virol. *69*, 2451–2461.

Braaten, D., and Luban, J. (2001). Cyclophilin A regulates HIV-1 infectivity, as demonstrated by gene targeting in human T cells. EMBO J. *20*, 1300–1309.

Bram, R.J., Hung, D.T., Martin, P.K., Schreiber, S.L., and Crabtree, G.R. (1993). Identification of the immunophilins capable of mediating inhibition of signal transduction by cyclosporin A and FK506: roles of calcineurin binding and cellular location. Mol. Cell. Biol. *13*, 4760–4769.

Brazin, K.N., Mallis, R.J., Fulton, D.B., and Andreotti, A.H. (2002). Regulation of the tyrosine kinase Itk by the peptidyl-prolyl isomerase cyclophilin A. Proc. Natl. Acad. Sci. USA *99*, 1899–1904.

Colgan, J., Asmal, M., Neagu, M., Yu, B., Schneidkraut, J., Lee, Y., Sokolskaja, E., Andreotti, A., and Luban, J. (2004). Cyclophilin A regulates TCR signal strength in CD4+ T cells via a proline-directed conformational switch in Itk. Immunity *21*, 189–201.

Duina, A.A., Chang, H.C., Marsh, J.A., Lindquist, S., and Gaber, R.F. (1996). A cyclophilin function in Hsp90-dependent signal transduction. Science *274*, 1713–1715.

Egger, D., Wolk, B., Gosert, R., Bianchi, L., Blum, H.E., Moradpour, D., and Bienz, K. (2002). Expression of hepatitis C virus proteins induces distinct membrane alterations including a candidate viral replication complex. J. Virol. *76*, 5974–5984.

El-Hage, N., and Luo, G. (2003). Replication of hepatitis C virus RNA occurs in a membrane-bound replication complex containing nonstructural viral proteins and RNA. J. Gen. Virol. *84*, 2761–2769.

Fischer, G., Tradler, T., and Zarnt, T. (1998). The mode of action of peptidyl prolyl cis/trans isomerases in vivo: binding vs. catalysis. FEBS Lett. *426*, 17–20.

Franke, E.K., Yuan, H.E., and Luban, J. (1994). Specific incorporation of cyclophilin A into HIV-1 virions. Nature *372*, 359–362.

Fuchsova, B., Novak, P., Kafkova, J., and Hozak, P. (2002). Nuclear